DOI: 10.1002/ejic.200600626

Cages on Surfaces: Thiol Functionalisation of Co^{III} Sarcophagine Complexes

Jack M. Harrowfield,[a,b] George A. Koutsantonis,*[b] Heinz-Bernhard Kraatz,[c] Gareth L. Nealon,[b] Grzegorz A. Orlowski,[c] Brian W. Skelton,[b] and Allan H. White[b]

Keywords: Sarcophagine / Amino acids / Disulfides / Cobalt / Self-assembled monolayers / Electrodeposition

A number of new (sarcophagine)cobalt compounds containing oligopeptide substituents terminated by a mercaptoethylamide unit, $[Co(R)(R')sar]_2^{6+}$ (R = NH_2, CH_3; R′ = NHpeptide-$CONHCH_2CH_2S$–), have been prepared utilising the carboxymethyl complexes $[Co(R)\{N(CH_2CO_2H)\}sar]^{3+}$ (R = NH_2, CH_3), and subsequently characterised. The amino acid residues, terminating with cystamine groups, were introduced into the carboxymethyl complexes using standard peptide coupling chemistry. The solid-state structures of $[Co(CH_3)\{N(CH_2CO_2H)\}sar]Cl_4\cdot H_2O$, $[Co(CH_3)\{N(CH_2CO_2H)_2\}sar]Cl_3\cdot 2H_2O$ and $[Co(CH_3)\{N(CH_2CO_2)_2\}sar]Cl\cdot 6.5H_2O$ were determined by single-crystal X-ray diffraction experiments, the first two forming lattices containing homochiral sheets of cations in planes parallel to [0,0,1]. In the structure of $[Co(CH_3)\{N(CH_2CO_2H)\}sar]Cl_4\cdot H_2O$, the cations are of the same absolute configuration, but this alternates from one sheet to the next. In the dihydrate, $[Co(CH_3)\{N(CH_2CO_2H)_2\}sar]Cl_3\cdot 2H_2O$, the structure appears to be very similar. The sheet alternation is different from the structure of the monohydrate, $[Co(CH_3)\{N(CH_2CO_2H)\}sar]Cl_4\cdot H_2O$. The deprotonated imidodiacetate complex, $[Co(CH_3)\{N(CH_2CO_2)_2\}sar]Cl\cdot 6.5H_2O$, was prepared in an unrelated reaction; the structure displays hydogen-bonding interactions involving the carboxylate groups and coordinated NH units. The solution electrochemistry of these compounds has been investigated using both cyclic voltammetry and differential pulse voltammetry. The compounds exhibited pH-dependent, quasi-reversible redox behaviour. A monolayer was prepared by the interaction of $[Co(R)sar(GlyNHCH_2CH_2S–)]_2^{6+}$ and a gold microelectrode using both conventional "self assembly" (SAM) and electrodeposition (EDM) techniques. Surface cyclic voltammograms were measured, which, after a period of induction associated with surface reorganisation, were typical of an ordered monolayer. The monolayer was characterised by XPS, showing peaks assigned to the presence of S, Co, N, O and C. Ellipsometry gave a film thickness of 7 ± 1 Å, consistent with the formation of a mono- rather than a multi-layer.

(© Wiley-VCH Verlag GmbH & Co. KGaA, 69451 Weinheim, Germany, 2007)

Introduction

Reagent immobilisation on surfaces is a sophisticated pathway to materials with a wide range of applications,[1,2] heterogeneous catalysis being one obvious application, such applications depending on the functionality introduced with the bound reagent, as well as upon the ease and convenience of the immobilisation procedure and the stability of the final product. Given the remarkable stability and varied electronic, magnetic and redox properties of metal complexes of the macrobicyclic polyamines known as "sarcophagines" (Figure 1),[3] these are species of particular appeal as entities for attachment to surfaces and for various related applications.[4] Reduction potentials for readily accessible species span a range of 2 V,[5] subject to modification in an interfacial environment,[6] and outer-sphere redox processes involving Co complexes are, for example, known to be rapid steps in reactions leading to photoinduced hydrogen production[7–10] and the reduction of oxygen to hydrogen peroxide.[11] Of practical importance in relation to immobilisation of such complexes is the facile synthesis of the ligand in forms with reactive "external" functional groups R (Figure 1).[12]

[a] Institut de Science et d'Ingénierie Supramoléculaires, Université Louis Pasteur,
8, allée Gaspard Monge, 67083 Strasbourg, France
Fax: +33-3-90245140
E-mail: harrowfield@isis.u-strasbg.fr
[b] Chemistry, M313, School of Biomedical, Biomolecular and Chemical Sciences, University of Western Australia,
Crawley 6009, Australia
Fax: +61-8-64887247
E-mail: gak@chem.uwa.edu.au
[c] Department of Chemistry, University of Saskatchewan,
110 Science Place, Saskatoon, S7N 5C9, Canada
Fax: +1-306-966-4730
E-mail: kraatz@skyway.usask.ca

Supporting information for this article is available on the WWW under http://www.eurjic.org or from the author.

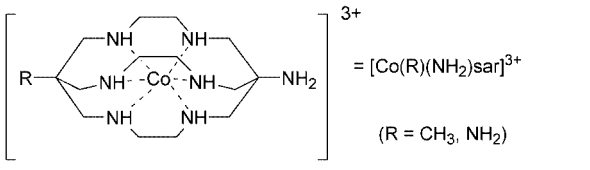

Cage = sarcophagine = "sar" = 3,6,10,13,16,19-hexaazabicyclo[6.6.6]icosane

Figure 1. Trivial nomenclature used throughout this work.

 © 2007 Wiley-VCH Verlag GmbH & Co. KGaA, Weinheim

Limited earlier work on surface-bound cage complexes has involved modification of electrodes by impregnation of thin Nafion films on graphite with simple cage complexes,[5] electropolymerisation of a thiophenylmethylamino cage complex on Pt,[12] and carbodiimide coupling of carboxyl groups on partially oxidised graphite to a diamino cage complex.[13] Amphiphilic cages[14,15] have also proved to have interesting biological properties, probably associated with their ability to be bound within membranes.[15] As a simple approach to the immobilisation of cage complexes on surfaces, we are currently exploring the use of the well-established surface chemistry of disulfides[1] to form monolayers of (sarcophagine)cobalt complexes on gold. This is based on the introduction of peptide substituents associated with cystamine units onto the cage, a facile synthesis when starting from readily synthesised glycylated derivatives.[16] The use of peptide-based tethering groups is advantageous as the length of the spacer between the surface and the cage moiety can be increased incrementally with relative ease, using common peptide synthetic techniques,[17] and tightly packed monolayers can be formed, presumably by hydrogen bonding between the amide groups.[18] A similar approach has been applied to the synthesis of ferrocene-decorated peptides as probes for elucidation of the mechanism(s) of electron transfer in proteins.[19]

Our immediate aim in the present work was to synthesise a series of disulfides bearing peptido cage complex substituents, evaluate their solution electrochemical characteristics, and determine a suitable method for their immobilisation onto gold electrodes. Because only a single disulfide substituent is required for surface tethering, our focus has been on obtaining derivatives of the monosubstituted cage complex $[Co(CH_3)(NH_2)sar]^{3+}$, though the more complicated syntheses of monofunctionalised derivatives of $[Co(NH_2)_2sar]^{3+}$ have also been investigated. These Co^{III} complexes exist in stable enantiomeric forms and thus the formation of diastereomeric forms of their oligopeptide derivatives was anticipated, though prior work suggested that differences between such diastereomers should be small.[12]

Results and Discussion

Synthesis

The primary amine group on a cage complex such as $[Co(NH_2)_2sar]^{3+}$ is a relatively poor nucleophile,[16] the proximity of the cationic metal centre diminishing this property, and, in cases where it is not convenient to use either the amine or an attacking electrophile in large excess, the cage complex is not an appropriate reagent for efficient synthesis, despite the fact that reactions of this type can be conducted.[13,20] Logically, it is more appropriate to use an electrophilic centre attached to the cage, because this property should be enhanced by the adjacent charge and indeed it is known that carboxymethyl derivatives of $[Co(NH_2)_2sar]^{3+}$ can be used efficiently in amide and peptide formation reactions.[21] Acceptably efficient carboxymethylation of $[Co(CH_3)(NH_2)sar]^{3+}$ (**1**) can be achieved under conditions involving reaction with a large excess of chloroacetate, which are similar to those used to obtain carboxymethyl derivatives of $[Co(NH_2)_2sar]^{3+}$.[16] Thus, the complexes $[Co(CH_3)(NHCH_2CO_2H)sar]^{3+}$ and $[Co(CH_3)\{N(CH_2CO_2H)_2\}sar]^{3+}$ were obtained as outlined in Scheme 1. These complexes, along with $[Co(NH_2)(NHCH_2CO_2H)sar]^{3+}$,[16] provided reactants to which standard peptide coupling methodologies could be applied to obtain derivatives incorporating cystamine residues as disulfide units linking two cages (Scheme 2).

In one reaction unrelated to peptide elaboration, crystals of the deprotonated diacid, $[Co(CH_3)\{N(CH_2CO_2)_2\}sar]^{+}$, were obtained (as the chloride) from an aqueous solution containing complex **3** held at a pH of approximately eight. We include below a discussion of the structure of this compound.

The syntheses produced mixtures that were readily separated by ion-exchange chromatography on Sephadex SP (using sodium citrate elution) due to the fact that the bis(cage) product has a charge of 6+ in neutral to basic solution, enabling facile discrimination between it and the less highly charged mono(cage) intermediate and any unreacted starting material.

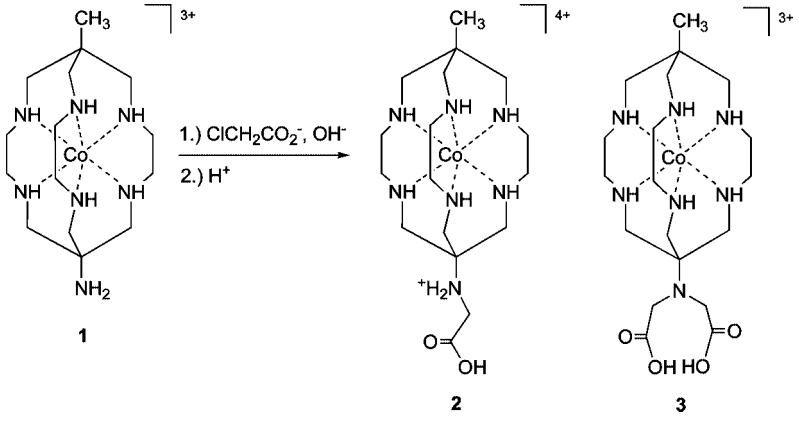

Scheme 1. Synthesis of carboxymethylated starting materials $[Co(CH_3)(NH_2CH_2CO_2H)sar]^{4+}$ (**2**) and $[Co(CH_3)\{N(CH_2CO_2H)_2\}sar]^{3+}$ (**3**).

 © 2007 Wiley-VCH Verlag GmbH & Co. KGaA, Weinheim

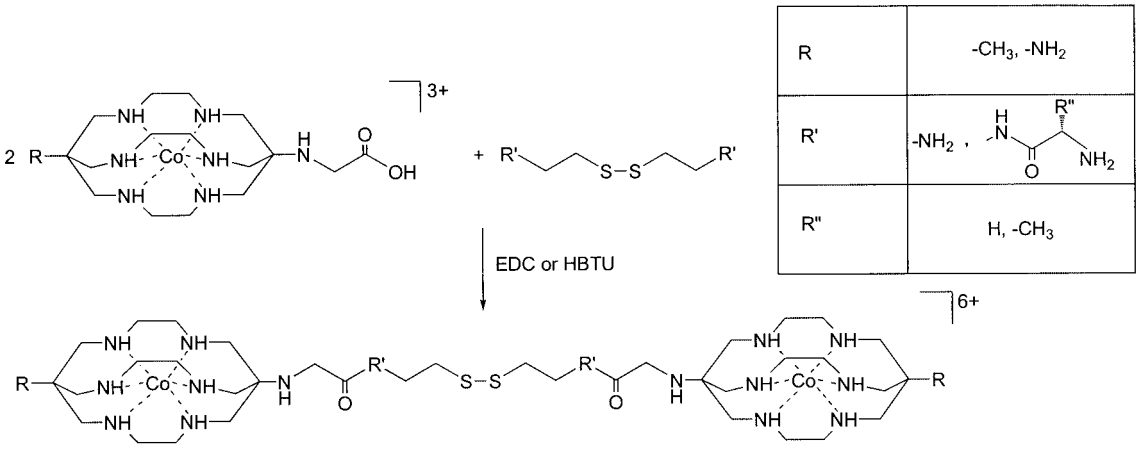

Scheme 2. Synthetic methodology used for the preparation of the disulfide complexes.

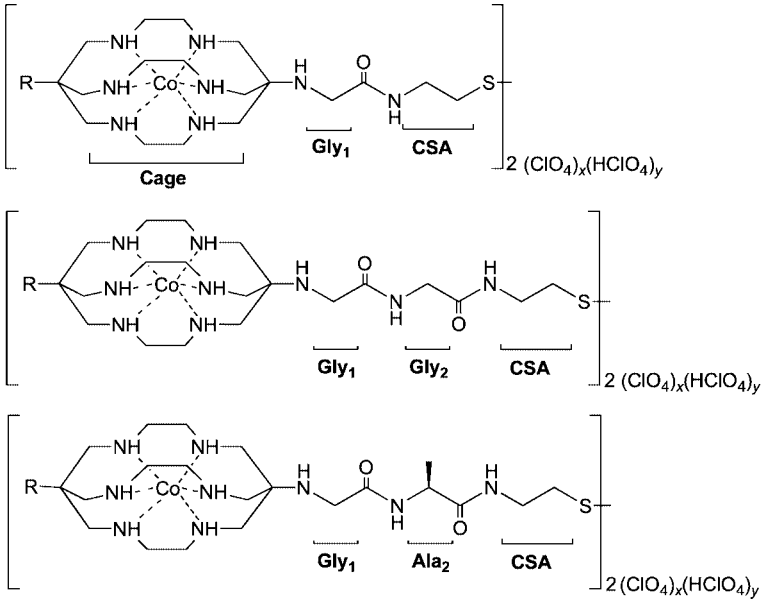

The method commonly employed to isolate Co^{III} complexes of the present type from Sephadex SP column eluates, including absorbing them on Dowex 50W strong acid resin, re-eluting with HCl and then concentrating to dryness,[16] proved to lead here to some hydrolysis of the peptides. Fortunately, the complexes could be readily isolated from the citrate eluates by precipitation as their very insoluble picrates. These could readily be converted into the perchlorates, preferred to the chlorides for electrochemical studies involving gold electrodes. It is worth noting that, despite the modest isolated yields reported for the compounds, the major band in the ion-exchange chromatography was always the disubstituted disulfide, indicating a relatively efficient reaction to give the desired product.

NMR Spectroscopy

All compounds synthesised (Table 1) exhibited NMR spectra consistent with their proposed structures. Evidence for the introduction of the carboxymethyl substituent to give the compounds **2** and **3** was observed with peaks between $\delta \approx 3.6$ and 3.7 ppm in their ^{1}H NMR and two peaks at $\delta = 43.6$, 52.5 ($-CH_2-$) and $\delta = 172.5$, 176.8 (C=O) ppm in their ^{13}C NMR spectra. The compounds **4**, **7** and **8** displayed a single amide –NH– peak ($\delta = 7.9$–8.0 ppm) in their ^{1}H NMR and a single C=O peak ($\delta \approx 170$ ppm) in their ^{13}C NMR spectra due to their CSA moieties. The compounds **5**, **6**, **9** and **10** displayed two peaks in both their ^{1}H NMR ($\delta = 7.8$–8.2 ppm) and ^{13}C NMR ($\delta = 168.7$–172.2 ppm) spectra, corresponding to the inequivalent NH and carbonyl centres of the amino acid (Gly or Ala) and CSA. The complex multiplets observed in the ^{1}H NMR spectra in the region between $\delta \approx 2$ and 3.5 ppm due to the methylene group resonances of the $[Co(CH_3)(NH_2)sar]^{3+}$ and $[Co(NH_2)_2sar]^{3+}$ moieties sometimes obscured other peaks corresponding to the Gly_1 $-CH_2-$ group and/or the $-CH_2-N$ group of CSA. The presence and position of the obscured peaks was deduced from the overall integration of the protons in this region, as well as cross-peaks observed in the 2D NMR experiments. ^{13}C NMR spectra reflected

 © 2007 Wiley-VCH Verlag GmbH & Co. KGaA, Weinheim

the complete asymmetry of the compounds, except for the compounds **8**, **9** and **10** in which two cage methylene signals were coincident. This was determined from the high intensity of the composite peak relative to the other cage methylene signals and by 2D NMR experiments. It is presumed that the use of racemic $[Co(CH_3)(NHCH_2CO_2H)sar]^{3+}$ as a reactant leads to the production of a mixture of *meso* and *rac* forms of the bis(cage) peptides but only in the case of compound **6** was any spectroscopic evidence for the presence of such a mixture obtained. The ^{13}C NMR spectrum of this complex shows some doubling of signals, similar to that observed in a dipeptide derivative of racemic $[Co(NH_2)(NHCH_2CO_2H)sar]^{3+}$.[21] This could reflect some racemisation of the amino acid during the synthesis but the product presently obtained by reaction of Δ-$[Co(NH_2)(NHCH_2CO_2H)sar]^{3+}$ with (L-Ala)$_2$CSA shows only sharp singlets in its ^{13}C NMR spectrum, indicating that this is not the case.

Table 1. List of compounds synthesised.

Compound	R	Cage	R′
2	$-CH_3$	racemic	–Gly-OH
3	$-CH_3$	racemic	$-N(CH_2CO_2H)_2$
4	$-CH_3$	racemic	–Gly-CSA-
5	$-CH_3$	racemic	–Gly-Gly-CSA-
6	$-CH_3$	racemic	–Gly-Ala-CSA-
7	$-NH_2$	racemic	–Gly-CSA-
8	$-NH_2$	Δ-enantiomer	–Gly-CSA-
9	$-NH_2$	Δ-enantiomer	–Gly-Gly-CSA-
10	$-NH_2$	Δ-enantiomer	–Gly-Ala-CSA-

Mass Spectrometry

Electrospray mass spectrometry (ESMS) has been recognised as a valuable method for obtaining molecular weights of cage complexes with little to no fragmentation.[22] ESMS spectra of compounds **2** and **3** display peaks consistent with the molecular ions corresponding to a loss of H^+ from the cation, and some peaks consistent with an additional association of chloride anions. ESMS spectra of compounds **4**–**10** in several cases display multiple peaks, corresponding to the molecular ion in charge states of 2+, 3+ and 4+, which are assigned as successive losses of H^+ from the parent ion, sometimes accompanied by association of a perchlorate anion. Loss of H^+ from a coordinated –NH– group of the cage is known and the resolution of the measurements here are sufficient to distinguish this possibility from that of Co^{III} reduction to Co^{II} in the mass spectrometer, as has also been observed.[22] There also appears to be no cleavage of the disulfide link during volatilisation.

Structure Determinations of Salts of Cations 2 and 3

The crystal structure determinations, modelled as $[Co(CH_3)(NH_2CH_2CO_2H)sar]Cl_4{\cdot}H_2O$, [**2**]$Cl_4{\cdot}H_2O$, $[Co(CH_3)\{N(CH_2CO_2H)_2\}sar]Cl_3{\cdot}2H_2O$, [**3**]$Cl_3{\cdot}2H_2O$, and $[Co(CH_3)\{N(CH_2CO_2)_2\}sar]Cl{\cdot}6.5H_2O$, [**3**–2H]$Cl{\cdot}6.5H_2O$ confirm the nature of the functionalisation (indicated by the given formulae) of the original cage complex $[Co(CH_3)(NH_2)sar]^{3+}$ expected on the basis of the method of synthesis and spectroscopic measurements; in the first two complexes, one, in the latter, two, formula units, devoid of crystallographic symmetry, comprise the asymmetric unit of the structure. The experimental details and refinement details are collected in Table 2, while structural representations showing the atom numbering schemes of the cations are given in Figure 2. Table 3 collects pertinent hydrogen-bonding data for the complexes. In [**2**]$Cl_4{\cdot}H_2O$, the O- and N-sites of the glycyl functional are both protonated, whereas in [**3**]$Cl_3{\cdot}2H_2O$, although a zwitterionic form is possible, the two carboxyl groups appear to retain their pro-

Table 2. Crystal data, details of data collection and structure refinement for the complexes.

Complex	[**2**]$Cl_4{\cdot}H_2O$	[**3**]$Cl_3{\cdot}2H_2O$	[**3**–2H]$Cl{\cdot}6.5H_2O$
Empirical formula	$C_{17}H_{40}Cl_4CoN_7O_3$	$C_{19}H_{43}Cl_3CoN_7O_6$	$C_{19}H_{50}ClCoN_7O_{10.5}$
M	591.3	639.9	639.0
Crystal system	triclinic	monoclinic	monoclinic
Space group	$P\bar{1}$	$P2_1/c$	$P2_1/c$
a [Å]	9.1450(7)	9.9703(5)	16.918(1)
b [Å]	11.4703(9)	9.9864(5)	14.243(1)
c [Å]	12.521(9)	27.8730(10)	25.024(2)
α [°]	83.594(1)	90	90
β [°]	87.671(1)	93.379(1)	103.099(5)
γ [°]	79.557(1)	90	90
V [Å^3]	1283.30(9)	2770.4(2)	5872.9(7)
$D_{calcd.}$ [g cm^{-3}]	1.53	1.51	1.445
Z	2	4	8
Size [mm]	$0.45\times0.37\times0.28$	$0.43\times0.43\times0.18$	$0.65\times0.40\times0.22$
μ_o [mm^{-1}]	1.12	0.96	0.74
Trans. (min./max.)	0.87	0.81	0.88
$2\Theta_{max.}$ [°]	64	70	63
N_t	17618	55294	154432
N ($R_{int.}$)	8747 (0.022)	11863 (0.37)	19162 (0.035)
N_o	7177	8958	15820
R	0.034	0.050	0.055
R_w (n_w)	0.073 (3.2)	0.095 (7)	0.102 (28)
T [K]	170	298	100

 © 2007 Wiley-VCH Verlag GmbH & Co. KGaA, Weinheim

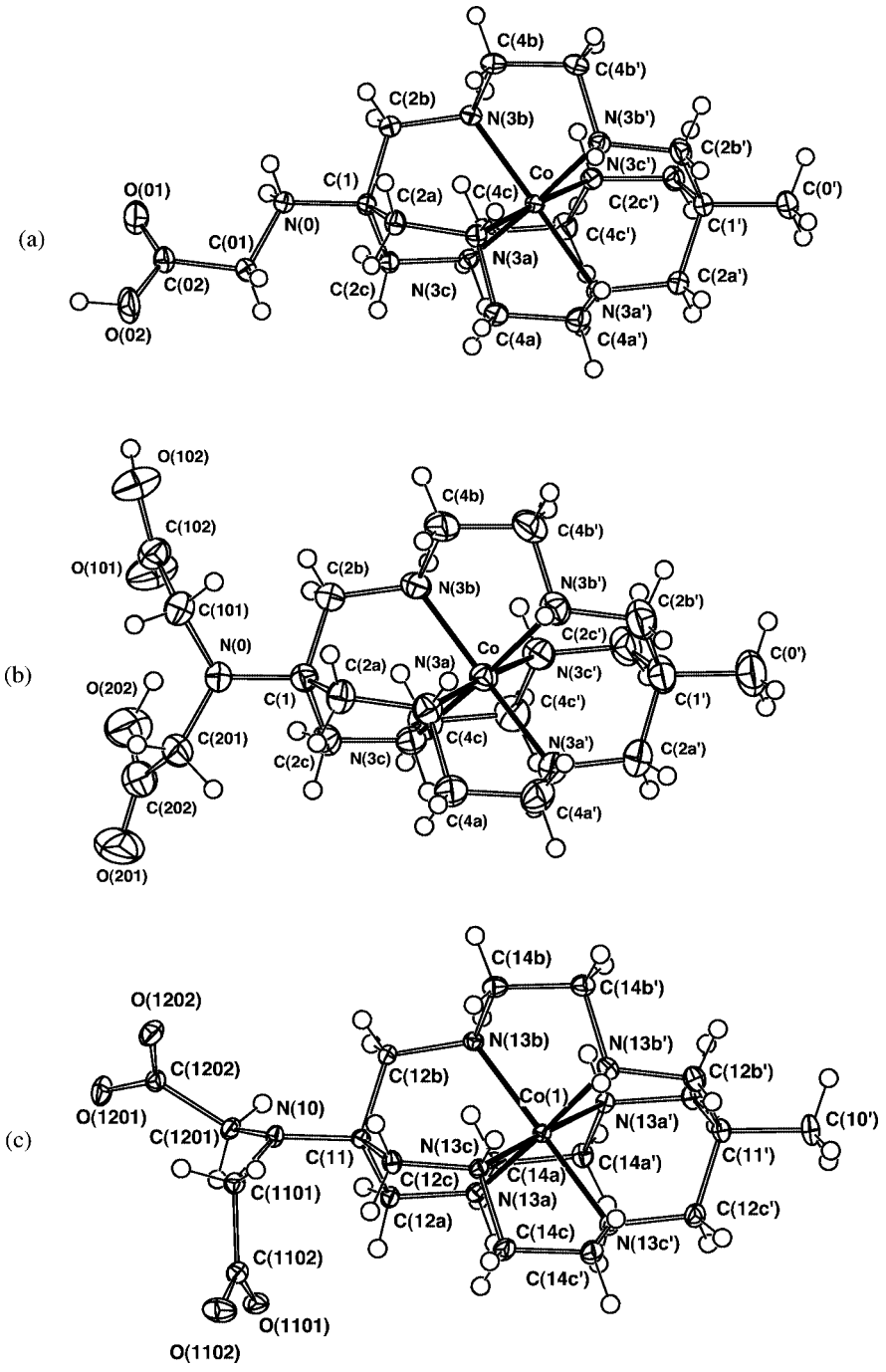

Figure 2. Structural representation of the cations in complexes (a) $[Co(CH_3)(NH_2CH_2CO_2H)sar]Cl_4{\cdot}H_2O$ [**2**]$Cl_4{\cdot}H_2O$, (b) $[Co(CH_3)\{N(CH_2CO_2H)_2\}sar]Cl_3{\cdot}2H_2O$, [**3**]$Cl_3{\cdot}2H_2O$ and (c) one of the two cations in $[Co(CH_3)\{N(CH_2CO_2)_2\}sar]Cl{\cdot}6.5H_2O$, [**3**–2H]$Cl{\cdot}6.5H_2O$. Probability ellipsoids shown at 50 [(a), (c)] and 20% (b) amplitude.

tons and the N-centre is unprotonated. This is despite the fact that the two complexes were isolated under essentially identical conditions from quite concentrated HCl solutions, though of course it need not be the case that the dominant species in solution are those which crystallise. The carboxylate groups are deprotonated in [**3**–2H]$Cl{\cdot}6.5H_2O$. All cation cores are of lel_3 conformation.

A view of the lattice of [**2**]$Cl_4{\cdot}H_2O$ along the *a* axis shows [Figure 3(a)], edge-on, sheets of cations lying in planes parallel to [0,0,1] which appear to form pairs separated by sheets of chloride ions. Within any given sheet, all cations are of the same absolute configuration, which alternates from one sheet to the next, and all adopt the lel_3 conformation. As has been discussed in detail elsewhere,[23] this conformation of amine cage complexes of Co^{III} is frequently associated with "hydrogen-bonding chelation" in which two coordinated NH centres on an open octahedral edge bind to the one unit, very commonly a chloride ion, just as is the case here [Figure 3(b)]. Each of the three chloride ions involved in such chelation by every cation has a third con-

 © 2007 Wiley-VCH Verlag GmbH & Co. KGaA, Weinheim

Table 3. Solution electrochemical data for compounds **2**–**10**. All $E_{1/2}$ values are referenced to the Ag/AgCl reference electrode. Scan rate 100 mV s^{-1}. Errors are the standard deviations from five measurements.

Compound	$E_{1/2}$ [V]	ΔE [V]	I_a/I_c
2	–0.552(2)	0.074(3)	1
3	–0.607(2)	0.073(2)	1
4	–0.565(3)	0.12(1)	1
5	–0.562(5)	0.09(1)	1
6	–0.563(2)	0.09(1)	0.9
7	–0.494(6)	0.118(5)	0.8
8	–0.497(2)	0.122(2)	0.8
9	–0.497(4)	0.116(5)	0.8
10	–0.496(5)	0.15(1)	0.8

tact at a similar or slightly shorter distance to oxygen, in two cases that of water molecules and in the third (the shortest of all contacts), that of a carboxyl group and specifically of its hydroxy unit. [The presence of the proton on the carboxyl group is clearly reflected in the asymmetry of the C–O distances of 1.198(2) and 1.327(3) Å.] The sheets of chloride ions which appear to separate the double sheets of cations contain this last "chelated" chloride ion plus the fourth chloride ion, which has one short contact [2.975(2) Å] to N of the pendent arm plus some rather remote CH contacts. Both can be considered as part of a centrosymmetric unit involving enantiomeric cations. It is also possible to identify centrosymmetric units linking the

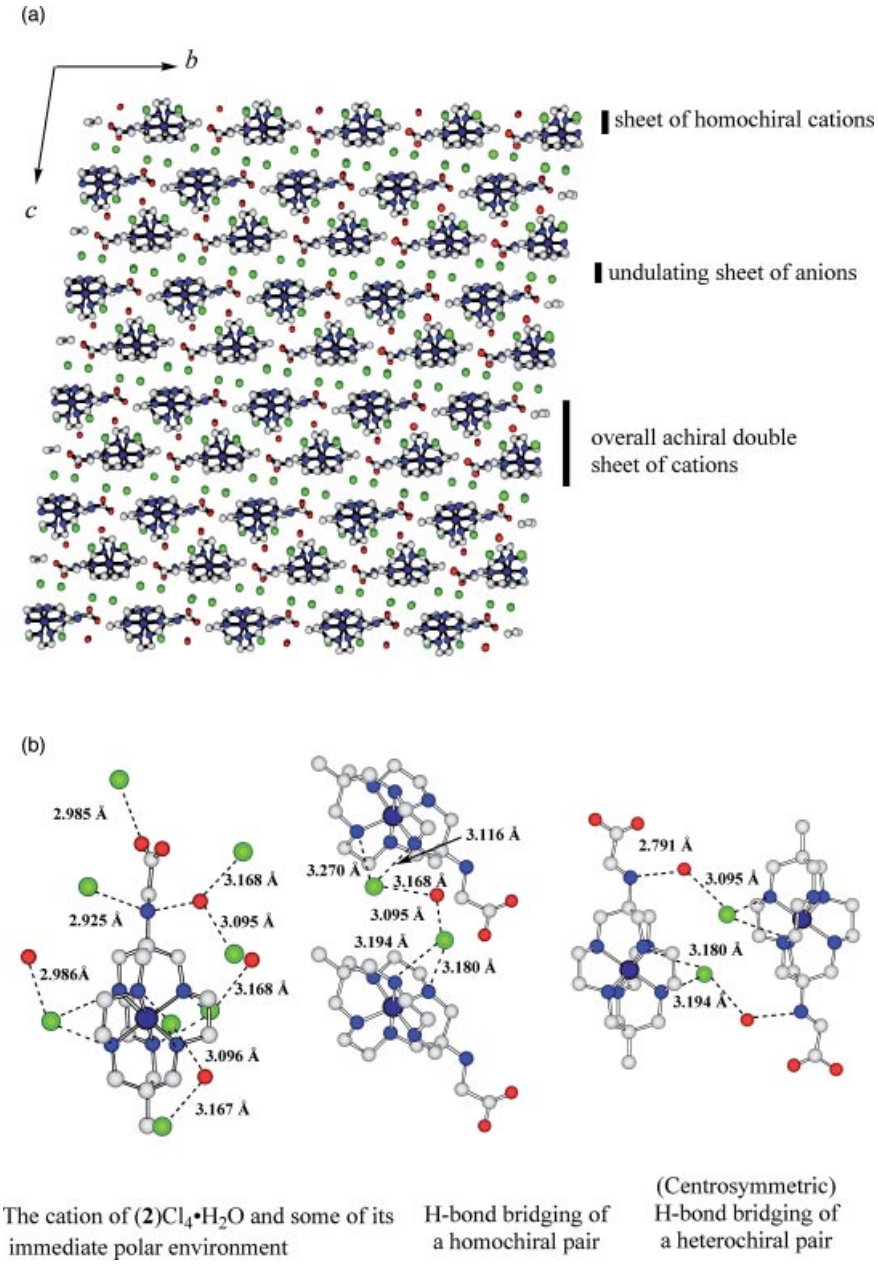

Figure 3. (a) View along the *a*-axis of the lattice of [Co(CH$_3$)(NH$_2$CH$_2$CO$_2$H)sar]Cl$_4$·H$_2$O, [**2**]Cl$_4$·H$_2$O; (b) representations of [Co(CH$_3$)(NH$_2$CH$_2$CO$_2$H)sar]Cl$_4$·H$_2$O, [**2**]Cl$_4$·H$_2$O, showing close contacts.

 © 2007 Wiley-VCH Verlag GmbH & Co. KGaA, Weinheim

double sheets where the water molecule and one of the chelated chloride ions with which it interacts provide hydrogen-bond bridges between the cations. The water molecule serves further as part of a hydrogen-bond network (involving its second chelated chloride neighbour) that links the homochiral columns of cations running parallel to the *a*-axis within any cation sheet. Hydrogen bonding, presumably to be regarded as "charge-assisted" within the formally ionic lattice, would appear to be the principal force determining the form of the lattice array.

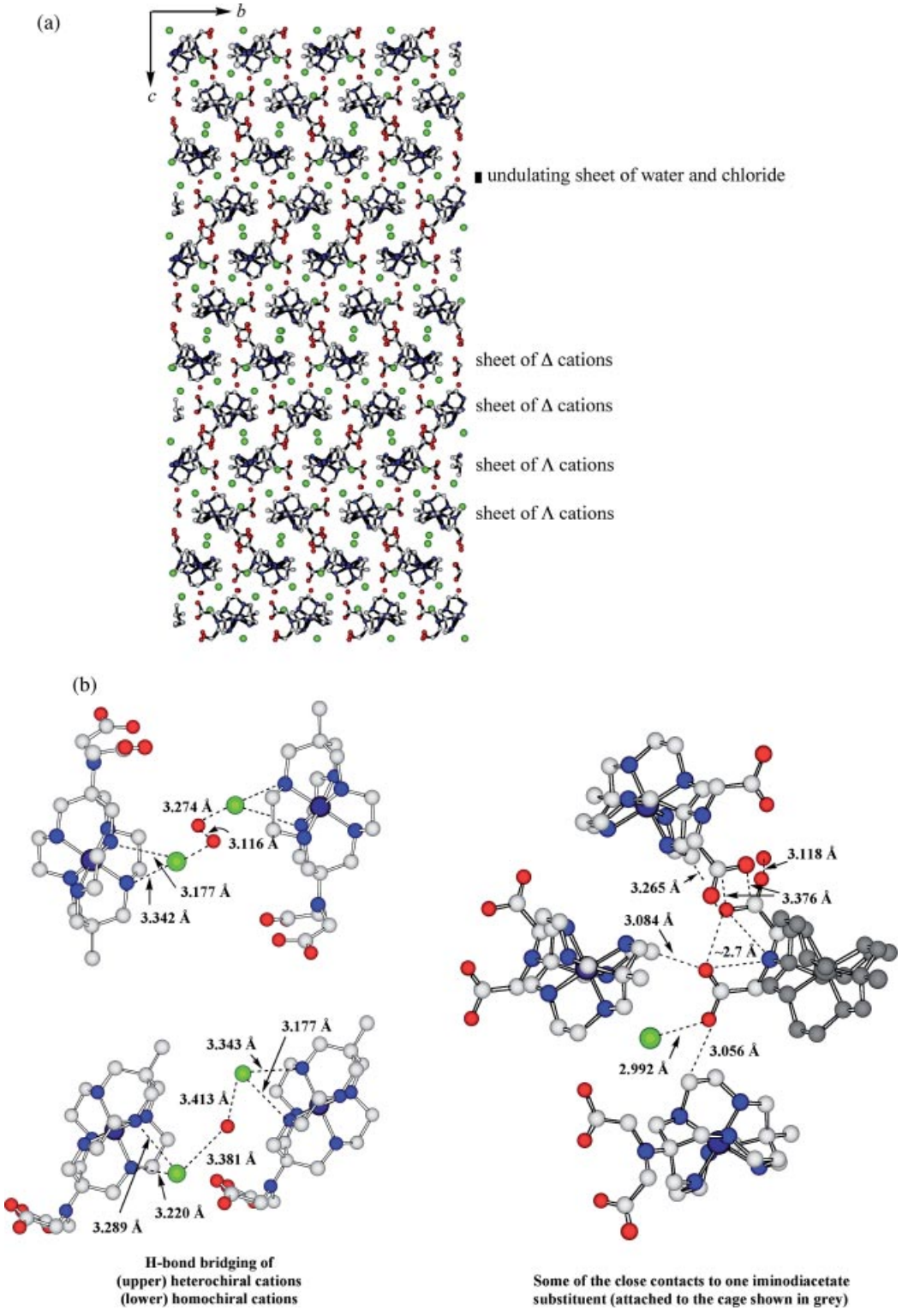

Figure 4. (a) Lattice of $[Co(CH_3)\{N(CH_2CO_2H)_2\}sar]Cl_3{\cdot}2H_2O$, **[3]**$Cl_3{\cdot}2H_2O$, along the *a*-axis; (b). Close contacts for $[Co(CH_3)\{N(CH_2CO_2H)_2\}sar]Cl_3{\cdot}2H_2O$, **[3]**$Cl_3{\cdot}2H_2O$.

 © 2007 Wiley-VCH Verlag GmbH & Co. KGaA, Weinheim

The lattice of $[Co(CH_3)\{N(CH_2CO_2H)_2\}sar]Cl_3{\cdot}2H_2O$, [**3**]$Cl_3{\cdot}2H_2O$, shows many close similarities to that of [**2**]-$Cl_4{\cdot}H_2O$ [Figure 4(a)]. When viewed again along the *a*-axis, homochiral cation sheets, parallel to [0,0,1], can be discerned edge-on and pairs of such sheets can be considered to be separated by undulating layers of chloride ions and water molecules. Such paired sheets are of opposite chirality, but sheets separated by the chloride/water layer are homochiral, so that the sheet alternation here is ...(Δ Λ)(Λ Δ)(Δ Λ)... and not ...Δ Λ Δ Λ Δ Λ... as in (**2**)$Cl_4{\cdot}H_2O$.

A network of conventional hydrogen bonds involving the NH, chloride and water entities serves to link cations of the same and opposite chirality but there is also more convincing evidence here that CH···O and even stacking interactions may play some role in the lattice construction [Figure 4(b)]. In this regard, the iminodiacetate pendent group in (**3**)$Cl_3{\cdot}2H_2O$ has several interesting features. The protons are clearly associated with O(*n*02), on the basis of difference map and geometrical evidence [C(102)–O(101, 202) 1.201(3), 1.309(3); C(202)–O(201, 202) 1.204(4), 1.314(4) Å]. The N-atom and the two "internal" O-atoms from separate carboxylate units form a nearly equilateral triangle ca. 2.7 Å on edge, indicating that one proton may in fact interact with all three, in a mode similar to that in which iminodiacetate can act as a tridentate ligand towards a metal ion. The external carboxyl hydroxy O-atom of the iminodiacetate entity has a relatively short contact [2.993(2) Å] to a chloride ion but is also within 3.056(3) Å of an ethylene bridge C-atom and within 3.470(4) Å of the methyl group carbon atom of different adjacent cations of the same chirality. The internal carboxyl carbonyl O-atom has, in addition to its N- and O-contacts mentioned above, two relatively short contacts [3.084(3), 3.184(3) Å] to carbon atoms of an ethylene bridge on another cation of the same chirality. The internal carboxyl hydroxy O-atom has a contact of 3.265(3) Å to a cap methylene C-atom, and the carboxyl group of which it is part lies in a plane parallel to that of another carboxyl group such that there are mutual C···O contacts (stacks?) of 3.376(3) Å, both these contacts involving an enantiomorphic cation. The external carboxyl carbonyl O-atom has a contact of 3.328(3) Å to an ethylene bridge C-atom and probably a more significant contact of 3.119(3) Å to a water oxygen atom which is hydrogen-bonded to a symmetry-related water molecule and thus connected to an enantiomorphic cation. The latter contacts, coupled to the stacking just mentioned, give rise to an infinite column parallel to *a*, linking sheets of both chiralities. In view of the nonlocation of the water molecule hydrogen atoms, and the lack of close contacts to other charged or polar components, reflected in (very) high displacement parameters for the residues assigned as oxygen atoms, hydrogen bonding plays a less dominant role in the lattice array seen for (**3**)$Cl_3{\cdot}2H_2O$ although clearly it remains a major influence.

In (**3**–2H)$Cl{\cdot}6.5H_2O$, the pendents are deprotonated, and devoid of any polar NH or OH hydrogen atoms; rather, the pendent groups themselves are now charged and are competitive with the halide ions (now deficient in numbers, there being only one per cation) in their interactions with the core NH sites and the water molecules. In each of the cations, one chloride ion is chelated between one pair of unprimed and primed NH groups from adjacent cage strings, one single carboxylate oxygen atom from the alternate cation of the asymmetric unit between a second, and a carboxylate pair, also from the alternate cation (symmetry-related) between the third. "Chelation" does not appear to impact on the carboxylate geometries in the manner that protonation does, there being no substantial distinction between the geometries of *O*,CO- and *O*,*O*C-chelated carboxylate groups, C–O tightly ranged between 1.252 and 1.265(3) [< > 1.258(4) Å], O–C–O similarly 123.6–124.7(2) [< > 124.1(5)°]. The interactions of each of the chloride ions are again {(chelate-H)$_2$ plus water molecule-H}. The interactions of the carboxylate oxygen atoms are such that

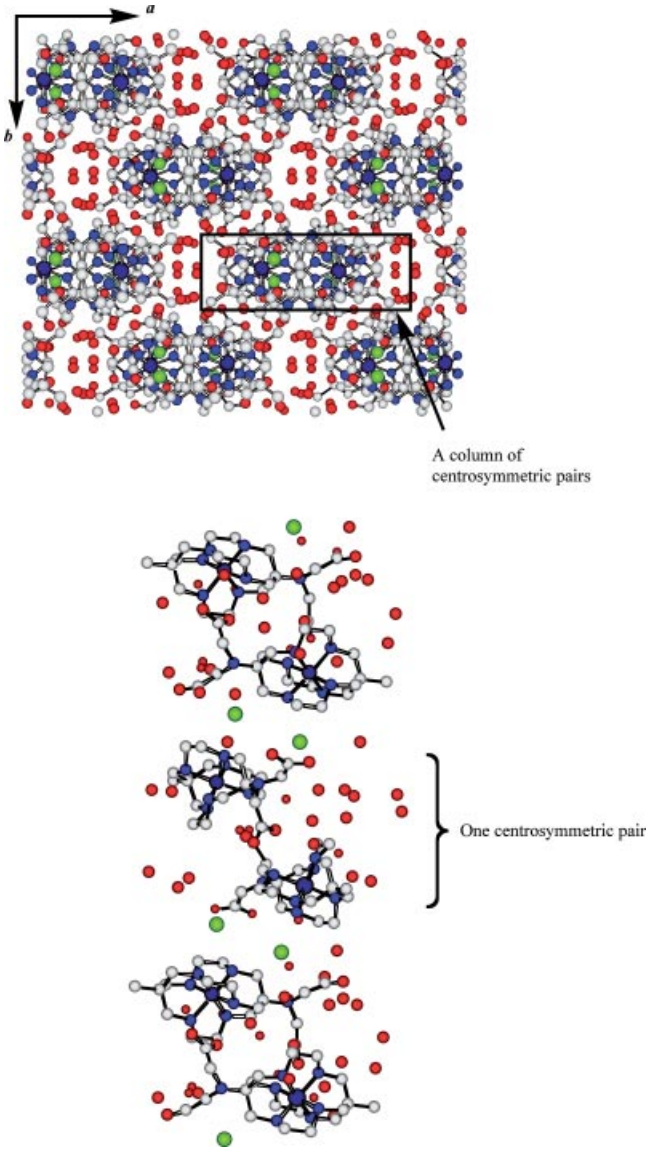

Figure 5. View of the unit cell of [**3**–2H]$Cl{\cdot}6.5H_2O$ along the *c*-axis (top) and perpendicular to one of the columns of the centrosymmetric pairs (bottom).

 © 2007 Wiley-VCH Verlag GmbH & Co. KGaA, Weinheim

each is associated with two hydrogen atoms: O(1101, 2201) are associated with/chelated by 2× NH, O(1202, 1202, 2102, 2102) are each associated with one NH group and one water molecule hydrogen atom, and O(1102, 2202) each with a pair of water molecule hydrogen atoms, the overall result being the formation of columns of centrosymmetric pairs of complex cations [Co(1)···Co(2) 8.3943(6) Å] along *c*; the pairs sandwich pairs of chloride ions, with associated Co(1)···Co(2) (*x*, 1½ – *y*, *z* – ½) 8.6617(6) Å involving cations of opposite chirality (Figure 5). A number of the water molecules (7, 9, 12, 13) are involved in hydrogen-donor interactions only to other water molecules, none forming aggregates in isolation, but, rather, linking the columns together.

Solution Electrochemistry

The solution electrochemistry of compounds **2**–**10** was investigated by cyclic voltammetry (CV) and differential pulse voltammetry (DPV) performed in aqueous solution using $NaClO_4$ as the supporting electrolyte, and selected data are presented in Table 3. Figure 6 depicts typical CV and DPV data for two of the complexes, **4** and **7**. The electrochemical behaviour of the compounds was found to be pH-sensitive and was often complicated by adsorption effects, particularly at Au or Pt working electrodes, which is consistent with previous work performed on the parent cages.[24] Adsorption behaviour at an Au electrode was confirmed by quartz crystal microbalance (QCM) measurements, whereby an increase in mass at the working electrode was observed at the potential corresponding to the pre-wave attributed to an adsorption phenomenon. In order to obtain reproducible results, the electrochemistry was performed in aqueous $NaClO_4$ adjusted to pH = 7.3 utilising a tris(hydroxymethyl)aminomethane (TRIS)/$HClO_4$ buffer. As the data in Table 3 show, the compounds display quasi-reversible redox behaviour, as determined from the ΔE values (> 0.059 V) and the peak current ratio I_a/I_c being lower than unity for most of the compounds. It is known that the $E_{1/2}$ values for the cages are sensitive to the nature of the apical substituents[24] and this is evident for the compounds synthesised here. The $E_{1/2}$ for compound **2** with one glycyl substituent is shifted by 55 mV to a more positive potential than that for compound **3**, which is terminated with an iminodiacetate moiety. The nature of the terminal group in compounds **4**–**10** also affects the $E_{1/2}$ value in that there is a significant shift (ca. 60–70 mV) to more positive potentials when the methyl group at the apex of the cage is replaced by an amino group. It is worth noting, however, that the $E_{1/2}$ value does not change when moving from the Gly-CSA to Gly-Gly-CSA and Gly-Ala-CSA derivatives if the group (–CH_3 or –NH_2) at the apex is held constant. This implies that changing the nature of the substituent beyond the initial –Gly- group does not affect the electronic environment about the Co centre and therefore explains the absence of any significant differences between diastereomers. The lack of an effect on the resulting $E_{1/2}$ value is important when considering the possible use of the complexes as electrocatalysts.

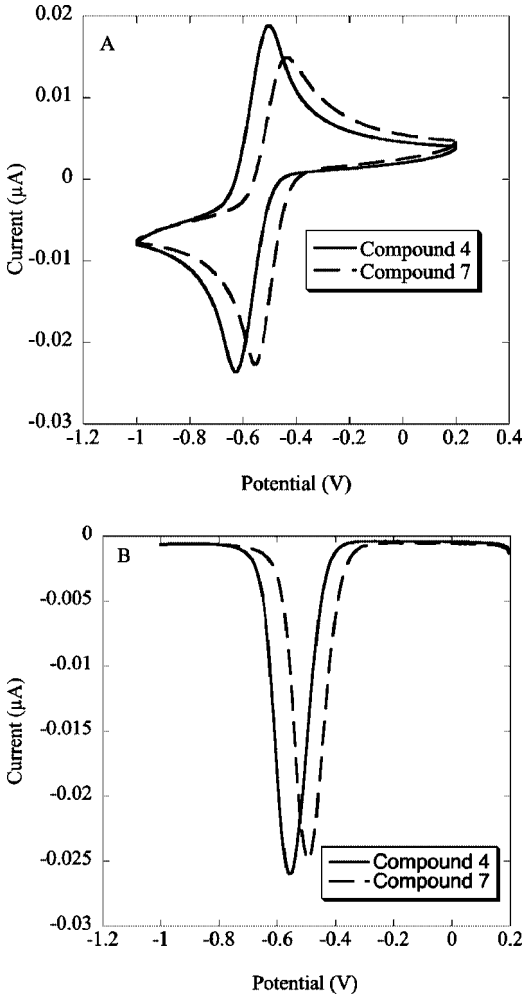

Figure 6. (a) Solution CVs of compounds **4** and **7** with GC working electrode at pH = 7.3, vs. Ag/AgCl (100 mV s^{-1}, 0.1 M $NaClO_4$). (b) DPVs of the reduction processes (scan rate 20 mV s^{-1}, pulse amplitude 50 mV).

Surface Electrochemistry

Preparation of gold microelectrodes modified by a film of one of the cage disulfides was achieved using both conventional "self-assembly" (SAM) by soaking the electrodes in aqueous solutions of the disulfides for 5 d, and by electrodeposition (EDM).[18] All surface cyclic voltammograms (CVs) were carried out in H_2O and in the presence of 2 M $NaClO_4$ as the supporting electrolyte in order to minimise the *iR* drop. Determination of the surface concentration of the cage was achieved by integration of the Faradaic peak currents of the cyclic voltammograms. Some of the characteristics of the film are shown in Table 4.

During repeated experiments it became clear that the films that formed immediately after the electrodeposition and washing steps displayed some unusual characteristics. CVs performed on the fresh films often displayed very small

 © 2007 Wiley-VCH Verlag GmbH & Co. KGaA, Weinheim

Table 4. Comparison of electrochemical data and surface coverage using ED and SA films for compound **4**. E_{fwhm} values reported for reduction waves. Values in parentheses indicate standard deviations from five measurements.

Technique	$E°$ [mV]	ΔE [mV]	I_a/I_c	E_{fwhm} [mV]	Specific area [Å^2]	Γ [mol cm^{-2}]
ED	–619(4)	56(8)	0.94(8)	195(12)	150(30)	$1.1(2) \times 10^{-10}$
SA	–602(20)	66(6)	0.84(4)	193(15)	150(40)	$1.2(3) \times 10^{-10}$

or unobservable current peaks corresponding to the cage species, and if they were present, the $E_{1/2}$ values were shifted to more negative potentials than the normal "equilibrium" potentials. It was found that repeated cycling of the potential, at scan rates from 0.1 to 10 V s^{-1}, for periods of up to and above 30 min produced CVs that displayed sharper and more intense peak currents, with a reduction in charging current (Figure 7). This effect could be explained by a random distribution of molecules on the surface at the start of the electrochemical experiment, which gradually changes to give a more ordered film. It is worth pointing out that the electrostatic repulsion between the cationic Co conjugates is likely to induce an initial disorder in the film as the Co headgroups maximise their physical separation. Electrochemical cycling might allow greater penetration of the anions into the film, and the enhanced charge neutrality would promote better packing within the film. As the film becomes more ordered, the Co centres become more thermodynamically homogeneous, which helps explain the reduction in peak half-widths during the experiment. A more ordered film would also help to explain the lower charging current observed with time, as a more effective "blocking layer" is formed. A similar effect has been observed in films produced from immobilised $Ni^{II/III}$ redox species[25] whereby a reduction in capacitive current and sharper Faradaic current peaks were observed with longer exposure times of the modified electrode to the disulfide solution. To interpret the results, the authors proposed a process whereby an initially random (disordered) film was replaced by a more ordered and compact film by replacement of surface molecules present in defective sites with fresh molecules in solution, whilst the total surface coverage (Γ) remained constant. Whilst replacement of surface-bound molecules with those in solution is clearly not possible here,

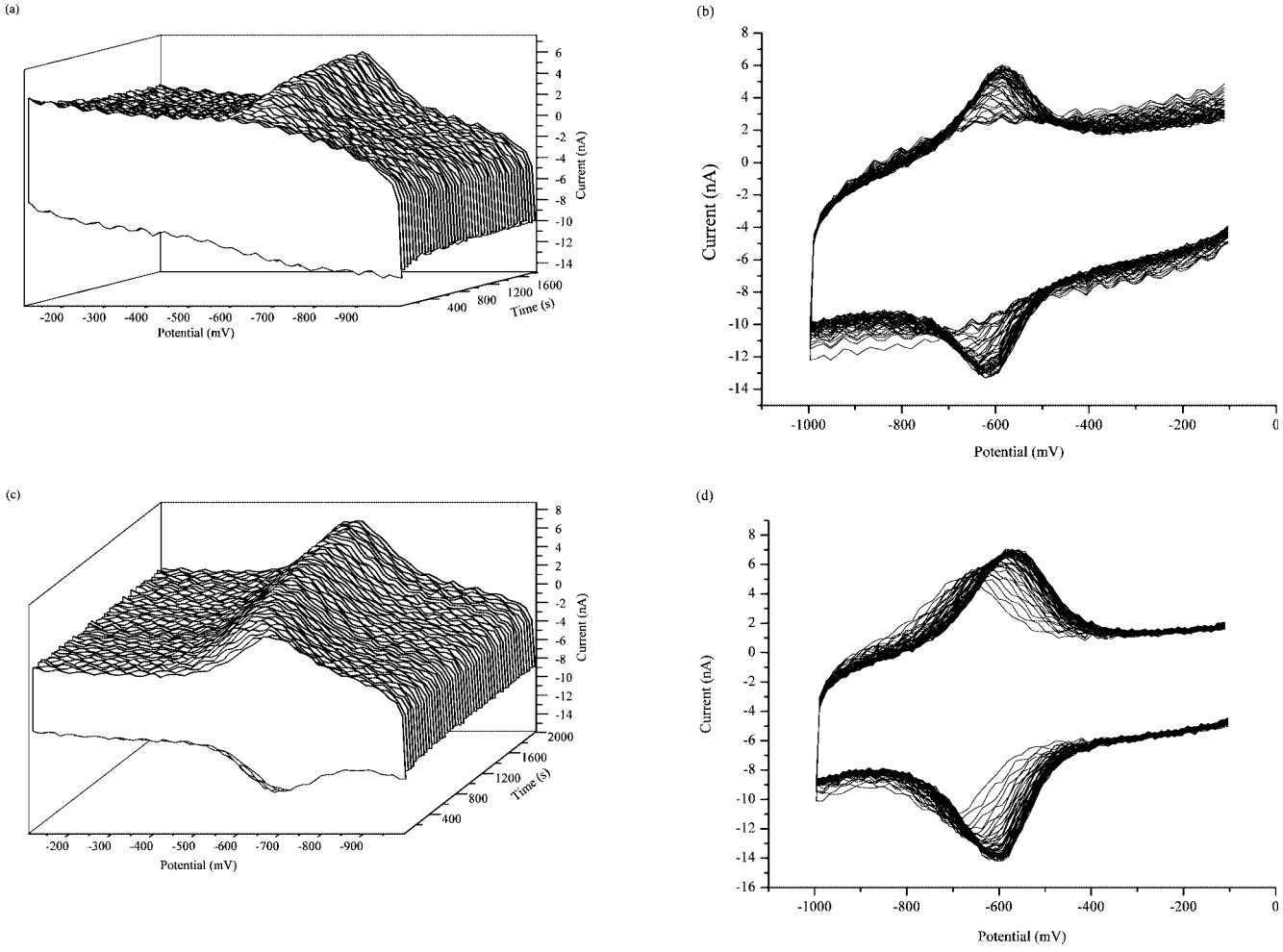

Figure 7. (a) Plot of repeated CVs vs. time for compound **4** immediately after ED and washing (10 V s^{-1}) [Note: Potential axis reversed for clarity in (a) and (c)]; (b) plot (a) viewed along the current/potential plane; (c): same as (a) but for SA; (d) plot (c) viewed along the current/potential plane.

 © 2007 Wiley-VCH Verlag GmbH & Co. KGaA, Weinheim

if a surface reorganisation effect is taking place, for example by surface migration of the gold thiolate molecules[26] or the potentially slow cleavage of the disulfide bond, the results between the two experiments would be almost identical. It is worth noting that this effect was more pronounced for the films produced by ED, when compared to those prepared by SA, and this phenomenon may be explained by the relative rates at which the two films are formed. Rapid film formation during ED might not allow the molecules enough time to orient themselves on the surface, which could be exacerbated by the negative potential "pulling" the cationic cage units to the surface, whereas the long time and lack of applied potential in SA would overcome and obviate these effects (Figure 8). Thus, in order to obtain stable and reproducible CVs, all freshly prepared films were subjected to the above electrochemical treatment before the determination of the electrochemical parameters shown in Table 4.

Plotting the peak current against scan rate for monolayers of compound **4** prepared using both SA and ED shows a linear relationship (Figure 9), which is expected for a surface-adsorbed species.[27] These results indicate the successful immobilisation of compound **4** onto the gold surface using both ED and SA techniques.

The stability of the monolayers was examined by repeated electrochemical cycling, from the open circuit potential (ca. –100 mV) to –1000 mV with a scan rate of 100 $V s^{-1}$ (Figure 10). The signal due to the reduction of the surface-bound Co^{III} conjugate shows virtually no loss in signal in-

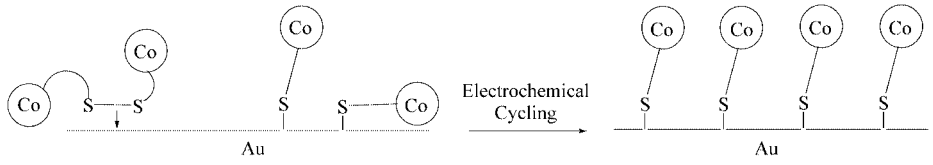

Figure 8. Diagram illustrating the possible reorganisation process leading to the observed increase in peak current and concomitant sharpening of peaks.

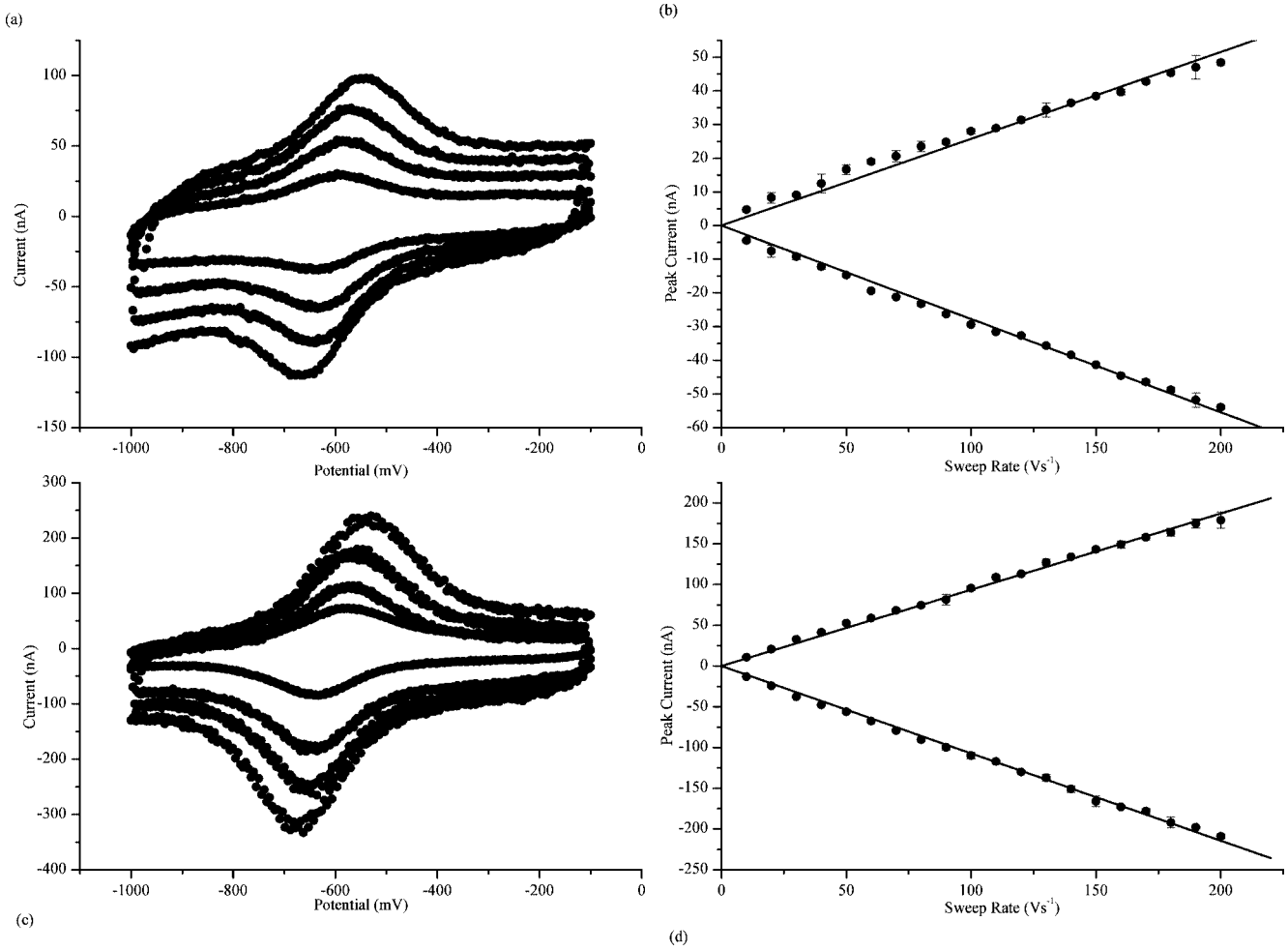

Figure 9. (a) CVs obtained at 50, 100, 150 and 200 $V s^{-1}$ for an EDM of compound **4**; (b) plot of peak current vs. scan rate for monolayer in plot (a); (c): as in plot (a) but for SAM; (d) as in plot (b) but for SAM.

 © 2007 Wiley-VCH Verlag GmbH & Co. KGaA, Weinheim

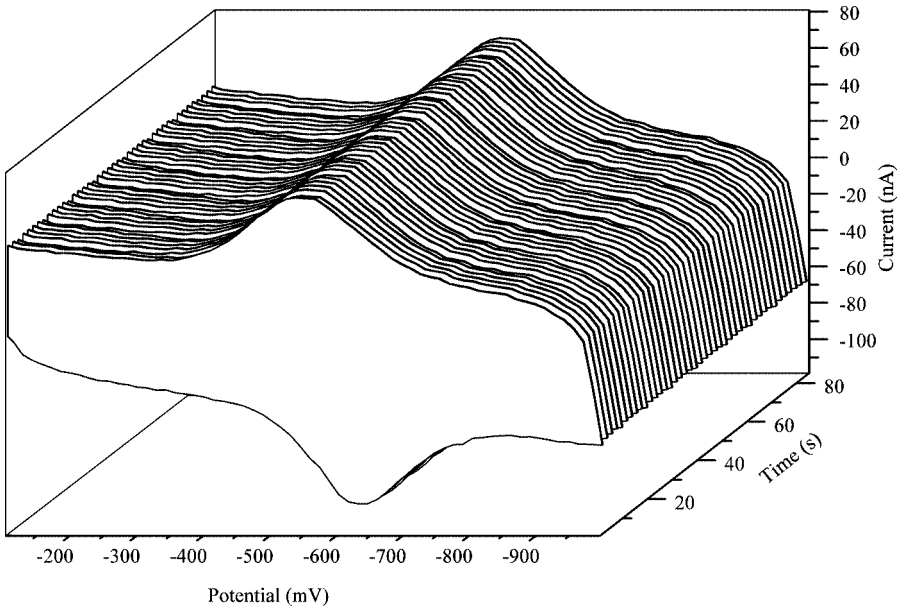

Figure 10. Repeated electrochemical cycling for film of compound **4** (100 $V s^{-1}$). (Note: Potential axis reversed for clarity.).

tensity upon repeated cycling for 100 s, indicating a stable monolayer has been formed.

As the data in Table 4 indicates, the monolayers formed using both the ED and SA techniques display very similar properties. The experimentally determined values for both films are virtually identical. Both films exhibit a reversible reduction of the Co^{III} cage at $E° = –619(4)$ mV vs. Ag/AgCl, which is anodically shifted compared to the solution electrochemistry. The peak separation is nonzero but significantly reduced compared to the solution electrochemistry, indicating potentially an increase in the reversibility of the process on the surface. This also signifies that there is some barrier for electron transfer through the spacer. As would be expected, the molecular footprint is larger than the more compact and neutral ferrocene conjugates.[18,28] This can be rationalised considering the electrostatic repulsion between the positively charged (sarcophagine)Co^{III} conjugates on the surface, and the large E_{fwhm} of ca. 200 mV is consistent with this, as theoretical treatments[29,30] predict a broadening of Faradaic peaks when the film consists of repulsive entities. However, it is important to point out that the footprint and thus the surface concentration for films deposited electrochemically and prepared by self-assembly are identical. All of the experimentally determined values for $E_{1/2}$, and importantly, the surface concentration and the related specific area of the molecule are in agreement between the two techniques. This shows that both methods can be used to generate monolayers of the compounds on a gold electrode.

SAMs of compound **4** on Au-coated silicon wafers were also prepared, displaying contact angles of 57(2)° (advancing) and 26(5)° (receding), indicating the presence of a polar

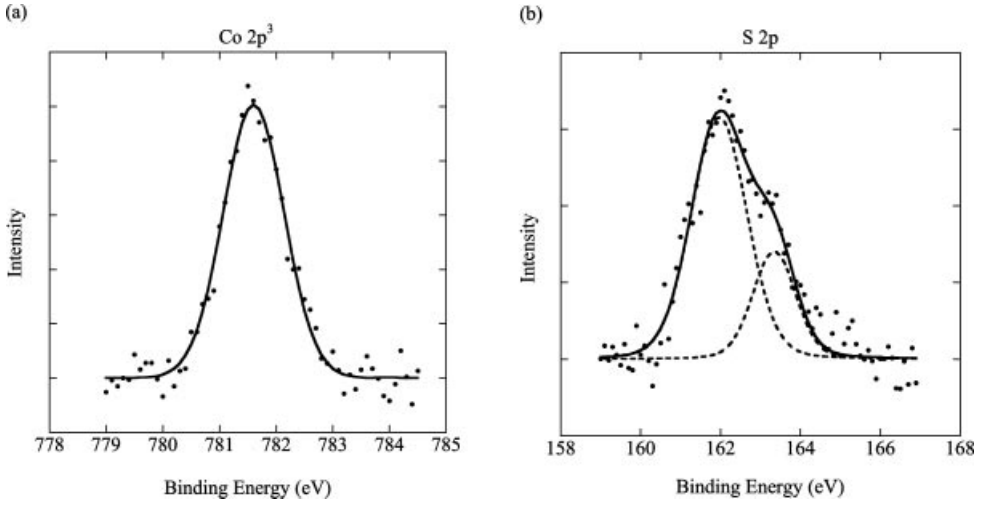

Figure 11. (a) XPS of the Co($2p^3$) region; (b) XPS of the S(2p) region. Closed circles represent experimental spectrum, solid line represents calculated spectrum and dashed lines indicate deconvoluted peaks.

 © 2007 Wiley-VCH Verlag GmbH & Co. KGaA, Weinheim

species on the surface. Evidence for a monolayer was obtained through the use of ellipsometry, which indicated a film thickness of (7 ± 1 Å) which is lower than the value expected for a fully extended molecule of compound **4** (ca. 15 Å). A low value for the film thickness could be due to the molecules lying at an angle to the surface and/or poor surface coverage, but it does suggest that the surface is modified by a monolayer and not a multilayer.

An XPS analysis of a SAM prepared on an Au-coated silicon substrate of compound **4** was undertaken in order to define the nature of the adsorption of the compound onto the gold surface. Disulfide chemisorption onto gold is generally believed to occur through a process in which the disulfide bond is broken to give two chemically independent molecules on the surface, bound as thiolates.[26] Peaks corresponding to S, Co, N, O and C are observed in the XPS spectrum which demonstrates the presence of compound **4** on the substrate. Figure 11 shows the major peak in the S(2p) region at 162 eV, which is consistent with the formation of an Au–S bond,[31] allowing us to conclude that the compound is bound as a thiolate on the surface. The Co binding energy of 781.5 eV is higher than the reported binding energy of 780.5 eV for the related $[Co(NO_2)_2sar]Cl_3$,[32] but does fall within the range of binding energy values for the Co^{III} N_6 complexes $[Co(en)_3]Cl_3$ and $[Co(NH_3)_6]Cl_3$ of 780.2–781.8 eV,[32,33] which indicates the cobalt atom is present as Co^{III}.

Conclusions

In this paper we have described the synthesis and solution electrochemical behaviour of a series of cobalt cage complexes bridged with short disulfide-containing peptides. In this way we have demonstrated the efficacy of this synthetic strategy which will allow us to tune "tail" length in a number of applications. We have also shown that it is possible, at least in one case, to immobilise a complex on a gold substrate utilising the disulfide linkage present. We believe that this undergoes facile cleavage to give initially species which lack ordering and subsequent electrochemical cycling allows them to attain thermodynamically stable surface ordering, although this phenomenon requires further study.

The surface attachment of these peptide-tethered sarcophagine complexes has allowed us to form modified surfaces containing redox-active centres and promise entry to an exciting range of applications.

Experimental Section

General: Nuclear magnetic resonance (NMR) spectra were acquired with a Bruker ARX 300 (^1H at 300 MHz and ^{13}C at 75.5 MHz), Bruker AV 500 (^1H at 500.13 MHz and ^{13}C at 125.8 MHz), or Bruker AV 600 (^1H at 600.13 MHz and ^{13}C at 150.9 MHz). Chemical shifts for samples measured in D_2O are expressed in ppm relative to an internal standard of acetone which was taken as being $\delta = 2.22$ ppm for ^1H NMR spectra and $\delta = 30.89$ ppm for ^{13}C NMR relative to TMS. Chemical shifts for samples measured in $[D_6]$DMSO were referenced to the residual solvent peak. Assignments were made with the aid of either the DEPT or HSQC techniques. Mass spectra were recorded using the electrospray technique (positive ion trap) with a VG Autospec instrument or QSTAR XL-MS/MS. Microanalyses for carbon, nitrogen and hydrogen were carried out by The Australian National University Microanalytical Service. All samples were thoroughly dried under vacuum at 50 °C for at least 4 h prior to their analysis. Ion exchange chromatography was performed under gravity flow using SP Sephadex C25 (Na^+ form, 200–400 mesh) or H^+ form Dowex 50Wx2 (200–400 mesh) cation exchange resin. Deionised water was used in all preparations. DMF was predried with molecular sieves (4 Å) prior to use. Dichloromethane was dried by distillation from CaH_2 and stored over molecular sieves (3 Å). Trisodium citrate (Na_3Cit) (Ajax), chloroacetic acid (Ajax), sodium picrate (BDH), *N*-[3-(dimethylamino)propyl]-*N*′-ethylcarbodiimide hydrochloride (EDC·HCl) (Aldrich), cystamine dihydrochloride (CSA·2HCl) (Aldrich), diisopropylethylamine (DIPEA) (Lancaster), *N*-hydroxysuccinimide (HOSu) (Aldrich), 2-benzotriazole-*N*,*N*,*N*,*N*,-tetramethyluronium hexafluorophosphate (HBTU) (Auspep), trifluoroacetic acid (TFA) (Aldrich), Boc-protected amino acids (Auspep), and trifluoromethanesulfonic (triflic) acid (Lancaster) were used as received. Solution electrochemical experiments were carried out at room temperature (23 ± 1 °C) with a MacLab Potentiostat or CHInstruments potentiostat model 660B or 440 in 0.1 M $NaClO_{4(aq)}$ adjusted to pH = 7.3 with tris(perchlorate) buffer, and an analyte concentration of 1 mM. A three-electrode cell system consisting of glassy carbon (BAS, 3.0 mm diameter) as the working electrode, Pt wire as the counter electrode and Ag/AgCl (3.0 M KCl) as the reference electrode was employed. The carbon electrodes were cleaned by polishing with a micro-cloth pad with Al_2O_3 slurry (0.05 μm) and washed thoroughly with water before use. For the cyclic voltametric (CV) studies the scan rate was 100 mV s^{-1} and for the DPV experiments a scan rate of 20 mV s^{-1} and pulse amplitude of 50 mV was used. Cyclic voltammograms (CVs) were scanned in the potential range of 0.2 to –1.0 V vs. Ag/AgCl. $[Co(CH_3)(NH_2)sar]Cl_3·HCl·0.5H_2O$,[34] *rac*- and Δ-$[Co(NH_2)(NH_2CH_2CO_2H)sar]Cl_3·2HCl$,[16] [Boc-Gly-CSA]$_2$ and [Boc-Ala-CSA]$_2$[35] were all synthesised as reported previously.

Structure Determinations: Full spheres of CCD area-detector diffractometer data were measured (ω-scans; monochromatic Mo-K_α radiation, $\lambda = 0.7107_3$ Å). $N_{t(otal)}$ reflections were obtained, these merging to N unique (R_{int} cited) after "empirical"/multiscan absorption correction (proprietary software), N_o with $F > 4\sigma(F)$ considered "observed" and used in the full-matrix least-squares refinements on F^2, refining anisotropic displacement parameter forms, $(x,y,z,U_{iso})_H$ being included constrained at estimates. Conventional residuals R, R_w {weights: $[\sigma^2(F^2) + n_wF^2]^{-1}$} are cited at convergence. Neutral atom complex scattering factors were employed within the context of the Xtal 3.7 program system.[36] Pertinent results are given above and in Tables 2 and 3 and Figure 2. In (**3**)$Cl_4·2H_2O$, a pair of substantial difference map residues were assigned as water molecule oxygen atoms, site occupancies unity after trial refinement, albeit with high displacement parameters, associated hydrogen atoms not being located. CCDC-605503 to -605505 contain the supplementary crystallographic data for this paper. These data can be obtained free of charge from The Cambridge Crystallographic Data Centre via www.ccdc.cam.ac.uk/data_request/cif.

Electrodeposition: All electrodeposition experiments were performed using a three-electrode cell system consisting of Au (25 μm diameter) as the working electrode, Pt wire as the counter electrode and Ag wire as the reference electrode. Electrodeposition was ac-

 © 2007 Wiley-VCH Verlag GmbH & Co. KGaA, Weinheim

complished by placing a freshly oxidised microelectrode (electrochemical cycling from –0.4 to +1.2 V vs. Pt wire in 0.5 M H_2SO_4) into a 1 mM solution of the analyte in 0.1 M $NaClO_{4(aq)}$ and applying –1.5 V for 30 min. After this period, the electrode was washed with water, then suspended in a vigorously stirred beaker of water for 10 min, and then 2 M $NaClO_{4(aq)}$ for 30 s. All electrochemical measurements were performed using a custom-built potentiostat in 2 M $NaClO_{4(aq)}$ using a three-electrode cell system consisting of Au (25 μm diameter) as the working electrode, Pt wire as the counter electrode and Ag/AgCl as the reference electrode, which was placed in a separate cell and connected to the analyte cell with a salt bridge (KNO_3). The electrochemical cell was enclosed in a grounded Faraday cage, and all electrolytes were degassed with a flow of $N_{2(g)}$ prior to the experiments, and an $N_{2(g)}$ blanket maintained throughout the course of the measurements. All electrochemical measurements were performed on at least five different microelectrodes to ensure reproducibility.

Self-Assembly: Monolayers were formed by soaking a freshly cleaned electrode (electrochemical cycling from –0.4 to +1.2 V vs. Pt wire in 0.5 M H_2SO_4) in a 1 mM aqueous solution of the complex for 5 d. After this period, the electrodes were treated exactly as above for the electrodeposited materials.

X-ray Photoelectron Spectroscopy: XPS measurements were performed using an Axis-165 X-ray Photoelectron Spectrometer (Kratos Analytical) with a monochromatic Al-K_a X-ray source (1486.7 eV). Survey spectra (0–1100 eV) were taken at constant analyser pass energy of 160 eV and high-resolution spectra of Au4f, C1s, N1s, O1s, S2p and Co2p, were acquired with a pass energy of 20 eV and a down time of 200 ms. The take-off angle measured as the angle between the film surface and the photoelectron energy analyser was 90°. The typical operating pressure in the analysing chamber was ca. $5 \cdot 10^{-10}$ Torr. Number of scans for high resolution required obtaining high signal/noise ratio varied from 4 for Au to 40 for Co, and 60 for S. The binding energies were referenced to Au4f7/2 at 84.0 eV.

[Co(CH$_3$)(NH$_2$CH$_2$CO$_2$H)sar]Cl$_4$·H$_2$O (2)Cl$_4$·H$_2$O and [Co(CH$_3$)-{N(CH$_2$CO$_2$H)$_2$}sar]Cl$_3$·2H$_2$O (3)Cl$_3$·2H$_2$O: [Co(CH$_3$)(NH$_2$)sar]-Cl_3·HCl·0.5H_2O (2.10 g, 4.0 mmol) was dissolved in H_2O (ca. 20 mL) in a three-necked round-bottomed flask, and the pH adjusted to ca. 10 by the addition of NaOH(aq). A solution of Na-CO_2CH_2Cl (25 g, 0.21 mol) in water (ca. 100 mL) was then added, and the pH again adjusted to ca. 10 by addition of more NaOH(aq). The solution was then heated at 80 °C under Ar(g) for 7 d, and the pH maintained at ca. 9–10 by dropwise addition of NaOH(aq). The reaction was monitored on micro-columns of Na^+ form SP C25 Sephadex by elution with 0.1 M Na_3Cit. More Na-CO_2CH_2Cl was added after 3 d (25 g, 0.21 mmol) and 5 d (10 g, 0.09 mmol), and after 7 d, the reaction mixture was acidified with acetic acid (pH < 5), diluted to 2 L in water, and applied to a column of H^+ form Dowex 50Wx2 cation exchange resin. The column was washed with water (500 mL), 1 M HCl (500 mL, to remove Na^+) and finally the products eluted with 3 M HCl. The fraction containing the products was then dried in the rotary evaporator, and the solid thus obtained dissolved into water (1 L) and applied to a column of Na^+ form Sephadex cation exchange resin. Elution with 0.05 M Na_3Cit produced three bands, the first being a minor yellow band, the second the major orange band, and the third a minor orange band. The three bands were applied to H^+ form Dowex 50Wx2 cation exchange resin separately, and treated with water (500 mL), 1 M HCl (500 mL) and eluted with 3 M HCl. The product from Band 1 was dried in a rotary evaporator, dissolved in hot water and precipitated by the addition of EtOH and finally Et_2O and cooling in the freezer. The product was collected by suction filtration, washed with a little cold EtOH, then finally Et_2O, and dried under vacuum to give (**3**)Cl_3·2H_2O (0.22 g, 0.35 mmol) as orange crystals. ^{1}H NMR (300 MHz, D_2O): δ = 0.9 (s, 3 H, –CH_3), 2.4–3.5 (m, 24 H, cage –CH_2–), 3.6 (s, 4 H, 2 iminodiacetate –CH_2–). ^{13}C NMR (75.5 MHz, D_2O): δ = 20.1 (–CH_3), 42.3 (C of methyl cage cap), 52.1 (cage –CH_2–), 52.5 (iminodiacetate –CH_2–), 54.4, 54.7, 55.2 (cage –CH_2–), 64.5 (C of amino cage cap), 176.8 (C=O). ES-MS: *m*/*z* = 243.64 [$C_{19}H_{39}CoN_7O_4$ – H^+]$^{2+}$, 486.21 [$C_{19}H_{39}CoN_7O_4$ – 2 H^+]$^+$, 522.22 [$C_{19}H_{39}CoN_7O_4$ – H^+ + $Cl^–$]$^+$. $C_{19}H_{43}Cl_3CoN_7O_6$ [(**3**)Cl_3·2H_2O, 630.88]: calcd. C 36.17, H 6.87, N 15.54; found C 36.49, H 6.52, N 15.70. Crystals of (**3**)Cl_3·2H_2O suitable for an X-ray structure determination were grown by slow concentration of a 2 M $HCl_{(aq)}$ solution of the complex. The product from Band 2 was treated as above for Band 1 to give (**2**)Cl_4·H_2O (1.26 g, 2.13 mmol) as orange crystals. ^{1}H NMR (500 MHz, D_2O): δ = 0.93 (s, 3 H, –CH_3), 2.4–3.5 (m, 24 H, cage –CH_2–), 3.69 (AB q, 2 H, Gly –CH_2–). ^{13}C NMR (126 MHz, D_2O): δ = 19.9 (–CH_3), 42.8 (C of methyl cage cap), 43.6 (Gly –CH_2–), 52.0, 55.1, 55.2, 55.3 (cage –CH_2–), 60.8 (C of amino cage cap), 172.5 (C=O). ES-MS: *m*/*z* = 464.21 [$C_{17}H_{37}CoN_7O_2$ – H^+ + $Cl^–$]$^+$, 428.23 [$C_{17}H_{37}CoN_7O_2$ – 2 H^+]$^+$, 500.16 [$C_{17}H_{37}CoN_7O_2$ + 2 $Cl^–$]$^+$. $C_{17}H_{40}Cl_4CoN_7O_3$ [(**2**)Cl_4·H_2O, 591.29]: calcd. C 34.53, H 6.82, N 16.58; found C 34.58, H 6.72, N 16.62. Crystals of (**2**)Cl_4·H_2O suitable for an X-ray structure determination were grown by slow concentration of a 2 M $HCl_{(aq)}$ solution of the complex. The triflate of [Co(CH$_3$)(NHCH$_2$CO$_2$H)sar]$^{3+}$ was obtained by dissolution of the chloride in neat triflic acid at ca. 50 °C whilst a constant stream of N_2 was bubbled though the solution for at least 1 h. The orange solution thus obtained was then cooled on ice and Et_2O added slowly with stirring to precipitate the triflate as a yellow-orange powder, which was collected by suction filtration and washed with copious quantities of Et_2O. The product from Band 3 was determined from ^{1}H NMR spectroscopy to be the starting material (0.35 g, 0.67 mmol).

[Co(CH$_3$)(Gly-NHCH$_2$CH$_2$S-)sar]$_2$(ClO$_4$)$_6$·HClO$_4$ (4)(ClO$_4$)$_6$·HClO$_4$: [Co(CH$_3$)(NH$_2$CH$_2$CO$_2$H)sar](CF$_3$SO$_3$)$_4$ (0.60 g, 0.58 mmol) was dissolved in DMF (30 mL), and *N*-hydroxysuccinimide (0.067 g, 0.58 mmol) was added to the orange solution, followed by DIPEA (0.4 mL, 2.3 mmol) and EDC·HCl (1.0 g, 5.2 mmol) and the orange mixture was stirred for 10 min. Cystamine dihydrochloride (CSA·2HCl) (0.063 g, 0.28 mmol) was then added, causing a precipitate to form immediately, which redissolved after ca. 10 min to give an almost clear solution. The mixture was stirred for 24 h, during which time a white precipitate had formed. The reaction mixture was then diluted into water (500 mL) and applied to a column of Na^+ form SP Sephadex SP 25 resin, which was washed with water (500 mL), then elution was commenced with 0.05–0.2 M Na_3Cit, which began to remove four bands, the fourth by far the major component. Band 4 was treated with a concentrated aqueous solution of sodium picrate (NaPic), until the precipitation of a very fine bright yellow solid ceased. The precipitate was collected on a sintered glass frit, at first by gravity, and then suction filtration. This material was washed well with water, and the moist yellow solid obtained was then suspended in water (ca. 100 mL) containing ca. 3 mL of concd. $HClO_{4(aq)}$, and to this was added EtOAc and the mixture stirred vigorously. Stirring was stopped periodically and the top layer of EtOAc decanted off and replaced with fresh solvent, until all of the solid had dissolved, leaving an orange aqueous phase, which was subsequently transferred to a separating funnel and extracted with EtOAc until the organic phase was colourless. The aqueous phase was then concentrated in a rotary evaporator until precipitation of an orange solid

 © 2007 Wiley-VCH Verlag GmbH & Co. KGaA, Weinheim

commenced, then placed on ice to complete the precipitation. The orange precipitate was collected on a sintered glass frit and washed with EtOH and then Et_2O and air-dried to give (**4**)$(ClO_4)_6$·$HClO_4$ (0.32 g, 0.19 mmol). The sample was recrystallised from warm H_2O/EtOH by the addition of Et_2O. ^1H NMR 600 MHz, [D_6]-DMSO): δ = 0.8 (s, 6 H, 2 $–CH_3$), 2.20–2.48 and 2.85–3.15 (m, 48 H, 2 cage $–CH_2–$), 2.53 (t, ca. 2 H, 2 cage pendent –NH–), 2.79 (t, 4 H, 2 $–CH_2–$S), 3.18 (m, 4 H, 2 Gly_1 $–CH_2–$), 3.39 (q, 4 H, 2 CSA $–CH_2–$N), 6.5 (br., 12 H, cage –NH–), 7.95 (t, 2 H, 2 CSA amide NH). ^{13}C NMR (151 MHz, [D_6]DMSO): δ = 19.5 ($–CH_3$), 37.0 (CSA $–CH_2–$S), 37.8 (CSA $–CH_2–$N), 42.1 (C of methyl cage cap), 44.3 (Gly_1 $–CH_2–$), 52.0, 53.5, 54.0, 54.2 (cage $–CH_2–$), 60.3 (C of amino cage cap), 171.0 (C=O). ES-MS: *m/z* = 486.22 [$C_{38}H_{82}Co_2N_{16}O_2S_2$ – 4 H^+]$^{2+}$. $C_{38}H_{83}Cl_7Co_2N_{16}O_{30}S_2$ [(**4**)$(ClO_4)_6$·$HClO_4$, 1674.32]: calcd. C 27.26, H 5.00, N 13.38; found C 27.43, H 5.38, N 13.31.

[Co(CH_3)(Gly-Gly-$NHCH_2CH_2S$-)sar]$_2(ClO_4)_6$·$HClO_4$·0.5H_2O (5)-$(ClO_4)_6$·$HClO_4$·0.5H_2O: [Co(CH_3)($NH_2CH_2CO_2H$)sar]$(CF_3SO_3)_4$ (0.80 g, 0.78 mmol) was dissolved in DMF (20 mL), and DIPEA (0.14 mL, 0.80 mmol) added, followed by *N*-hydroxysuccinimide (0.138 g, 1.20 mmol), followed by HBTU (0.445 g, 1.17 mmol) and the orange solution was stirred for 20 min. In a separate round-bottomed flask, Boc-Gly-CSA (0.177 g, 0.380 mmol) was dissolved in CH_2Cl_2 (3 mL) containing TFA (1.5 mL) and the solution stirred for 1 h, during which time, an oily material separated from the mixture. The solvents were removed under reduced pressure, and the oily residue redissolved in DMF (6 mL) containing an excess of DIPEA (0.36 mL), and then added to the orange cage solution, which was then stirred at room temp. for 18 h. The workup procedure was identical to that of compound **4** above, to give (**5**)-$(ClO_4)_6$·$HClO_4$·0.5H_2O as an orange solid (0.43 g, 0.24 mmol). The sample was recrystallised from warm H_2O by the addition of EtOH, to give an orange oil which solidified upon standing at room temp. for several hours. ^1H NMR (600 MHz, [D_6]DMSO): δ = 0.80 (s, 6 H, 2 $–CH_3$), 2.20–2.50 and 2.85–3.15 (m, 48 H, 2 cage $–CH_2–$), 2.60 (t, 2 H, 2 cage pendent –NH–), 2.76 (t, 4 H, 2 $–CH_2–$S), 3.21 (dq, 4 H, 2 Gly_1 $–CH_2–$), 3.36 (m, 4 H, 2 CSA $–CH_2–$N), 3.73 (d, 4 H, 2 Gly_2 $–CH_2–$), 6.51 (br. s, 6 H, 2 cage NH), 6.56 (br. s, 6 H, 2 cage NH), 8.00 (t, 2 H, 2 Gly_2 amide NH), 8.08 (t, 2 H, 2 CSA amide NH). ^{13}C NMR (151 MHz, [D_6]DMSO): δ = 19.5 ($–CH_3$), 36.9 (CSA $–CH_2–$S), 38.0 (CSA $–CH_2–$N), 41.5 (Gly_2 $–CH_2–$), 42.1 (C of methyl cage cap), 44.3 (Gly_1 $–CH_2–$), 52.1, 53.6, 54.0, 54.1 (cage $–CH_2–$), 60.3 (C of amino cage cap), 168.9, 171.2 (C=O). ES-MS: *m/z* = 362.51 [$C_{42}H_{88}Co_2N_{18}O_4S_2$ – 3 H^+]$^{3+}$, 395.83 [$C_{42}H_{88}Co_2N_{18}O_4S_2$ – 2 H^+ + ClO_4^-]$^{3+}$, 272.13 [$C_{42}H_{88}Co_2N_{18}O_4S_2$ – 2 H^+]$^{4+}$, 543.25 [$C_{42}H_{88}Co_2N_{18}O_4S_2$ – 4 H^+]$^{2+}$. $C_{42}H_{90}Cl_7Co_2N_{18}O_{32.5}S_2$ [(**5**)$(ClO_4)_6$·$HClO_4$·0.5H_2O, 1797.43]: calcd. C 28.06, H 5.05, N 14.03; found C 28.14, H 5.43, N 13.99.

[Co(CH_3)(Gly-Ala-$NHCH_2CH_2S$-)sar]$_2(ClO_4)_6$·$HClO_4$·H_2O (6)-$(ClO_4)_6$·$HClO_4$·H_2O: The procedure used was the same as that for compound **5** above. From [Co(CH_3)($NH_2CH_2CO_2H$)sar]-$(CF_3SO_3)_4$ (0.86 g, 0.84 mmol), DMF (15 mL), DIPEA (0.15 mL, 0.86 mmol + 0.5 mL, 3 mmol), *N*-hydroxysuccinimide (0.11 g, 0.96 mmol), HBTU (0.35 g, 0.92 mmol), Boc-Ala-CSA (0.20 g, 0.40 mmol), was obtained (**6**)$(ClO_4)_6$·$HClO_4$·H_2O (0.36 g, 0.20 mmol). The sample was recrystallised from warm H_2O by the addition of EtOH. ^1H NMR (600 MHz, [D_6]DMSO): δ = 0.79 (s, 6 H, 2 cage $–CH_3$), 1.22 (d, 6 H, 2 Ala $–CH_3$), 2.20–2.50 and 2.85–3.15 (m, 48 H, 2 cage $–CH_2–$), 2.56 (AB q, 2 H, 2 cage pendent –NH–), 2.76 (m, 4 H, 2 $–CH_2–$S), 3.17 (m, 4 H, 2 Gly_1 $–CH_2–$), 3.25–3.50 (m, 4 H, 2 CSA $–CH_2–$N), 4.28 [sext, 2 H, Ala_2 –CHα–), 6.51 (br. s, 6 H, 2 cage –NH–), 6.56 (br. s, 6 H, 2 cage –NH–), 7.85 (d, 2 H, 2 Ala_2 amide NH), 8.16 (t, 2 H, 2 CSA amide NH). ^{13}C NMR (151 MHz, [D_6]DMSO): δ = 18.9 (Ala $–CH_3$), 19.5 (cage $–CH_3$), 36.9 (CSA $–CH_2–$S), 37.9 (CSA $–CH_2–$N), 42.0 (C of methyl cage cap), 44.4 (Gly_1 $–CH_2–$), 47.7 (Ala_2 –CHα–), 52.2, 53.6, 53.9, 54.0 (cage $–CH_2–$), 60.2 (C of amino cage cap), 170.1, 172.1 (C=O). Note: Some peaks were doubled due to the presence of *meso* and *rac* compounds but these doubled peaks are reported with a single chemical shift in order to simplify the analysis of the spectra. ES-MS: *m/z* = 371.85 [$C_{44}H_{92}Co_2N_{18}O_4S_2$ – 3 H^+]$^{3+}$, 557.27 [$C_{44}H_{92}Co_2N_{18}O_4S_2$ – 4 H^+]$^{2+}$. $C_{44}H_{95}Cl_7Co_2N_{18}O_{33}S_2$ [(**6**)$(ClO_4)_6$·$HClO_4$·H_2O, 1834.49]: calcd. C 28.81, H 5.22, N 13.74; found C 28.82, H 5.41, N 13.69.

[Co(NH_2)(Gly-$NHCH_2CH_2S$-)sar]$_2(ClO_4)_6$·$HClO_4$·2H_2O (7)-$(ClO_4)_6$·$HClO_4$·2H_2O: The procedure used was the same as that for compound **4** above. From [Co(NH_3)($NH_2CH_2CO_2H$)-sar]$(CF_3SO_3)_5$ (2.55 g, 2.16 mmol), DMF (15 mL), DIPEA (0.76 mL, 4.4 mmol + 0.5 mL, 3 mmol), *N*-hydroxysuccinimide (1.01 g, 8.8 mmol), EDC·HCl (1.7 g, 8.9 mmol), CSA·2HCl (0.22 g, 1.0 mmol), was obtained (**7**)$(ClO_4)_6$·$HClO_4$·2H_2O (0.45 g, 0.26 mmol). The sample was recrystallised from warm H_2O by the addition of EtOH. ^1H NMR (600 MHz, [D_6]DMSO): δ = 1.72 (br., 4 H, 2 $–NH_2$), 2.25–2.50 and 2.75–3.20 (m, 48 H, 2 cage $–CH_2–$), 2.53 (t, 1 H, 2 Gly_1 –NH–), 2.79 (t, 4 H, 2 $–CH_2–$S), 3.16 (m, 4 H, 2 Gly_1 $–CH_2–$), 3.39 (q, 4 H, 2 CSA $–CH_2–$N), 6.53 (br. s, 6 H, 2 cage NH), 6.59 (br. s, 6 H, 2 cage NH), 7.95 (t, 2 H, 2 CSA amide NH). ^{13}C NMR (151 MHz, [D_6]DMSO): δ = 37.0 ($–CH_2–$S), 37.7 (CSA $–CH_2–$N), 44.3 (Gly_1 $–CH_2–$), 52.1, 54.0, 54.1, 54.5 (cage $–CH_2–$), 56.9, 60.3 (cage C), 170.9 (Gly_1 C=O). ES-MS: *m/z* = 325.15 [$C_{36}H_{80}Co_2N_{18}O_2S_2$ – 3 H^+]$^{3+}$, 244.12 [$C_{36}H_{80}Co_2N_{18}O_2S_2$ – 2 H^+]$^{4+}$, 487.22 [$C_{36}H_{80}Co_2N_{18}O_2S_2$ – 4 H^+]$^{2+}$, 358.47 [$C_{36}H_{80}Co_2N_{18}O_2S_2$ – 2 H^+ + ClO_4^-]$^{3+}$. $C_{36}H_{85}Cl_7Co_2N_{18}O_{32}S_2$ [(**7**)$(ClO_4)_6$·$HClO_4$·2H_2O, 1712.33]: calcd. C 25.25, H 5.00, N 14.72; found C 25.44, H 4.87, N 14.57.

Δ-[Co(NH_2)(Gly-$NHCH_2CH_2S$-)sar]$_2(ClO_4)_6$·$HClO_4$·2H_2O (8)-$(ClO_4)_6$·$HClO_4$·2H_2O: The procedure used was the same as that for compound **4** above. From [Co(NH_3)($NH_2CH_2CO_2H$)sar]Cl_5·3H_2O (0.50 g, 0.75 mmol), DMF (15 mL), DIPEA (0.26 mL, 1.5 mmol + 0.5 mL, 3 mmol), *N*-hydroxysuccinimide (0.17 g, 1.5 mmol), EDC·HCl (0.29 g, 1.5 mmol), CSA·2HCl (0.084 g, 0.37 mmol), was obtained (**8**)$(ClO_4)_6$·$HClO_4$·2H_2O (0.42 g, 0.24 mmol). The sample was recrystallised from warm H_2O by the addition of EtOH. ^1H NMR (600 MHz, [D_6]DMSO): δ = 2.40–2.65 and 2.90–3.35 (m, 48 H, 2 cage $–CH_2–$), 2.79 (t, 4 H, 2 $–CH_2–$S), 3.17 (m, 4 H, 2 Gly_1 $–CH_2–$), 3.41 (q, 4 H, 2 CSA $–CH_2–$N), 6.57 (br. s, 6 H, 2 cage –NH–), 6.84 (br. s, 6 H, 2 cage –NH–), 7.97 (t, 2 H, 2 CSA amide NH), 8.36 (br. s, 4 H, 2 free $–NH_2$). ^{13}C NMR (151 MHz, [D_6]-DMSO): δ = 36.9 (CSA $–CH_2–$S), 37.8 (CSA $–CH_2–$N), 44.3 (Gly_1 $–CH_2–$), 50.9, 52.1, 53.6 (2 C) (cage $–CH_2–$), 55.6, 60.5 (C), 170.2 (C=O). ES-MS: *m/z* = 244.16 [$C_{36}H_{80}Co_2N_{18}O_2S_2$ – 2 H^+]$^{3+}$, 358.51 [$C_{36}H_{80}Co_2N_{18}O_2S_2$ – 2 H^+ + ClO_4^-]$^{3+}$. $C_{36}H_{85}Cl_7Co_2N_{18}O_{32}S_2$ [(**8**)$(ClO_4)_6$·$HClO_4$·2H_2O, 1712.33]: calcd. C 25.25, H 5.00, N 14.72; found C 24.99, H 5.02, N 14.35.

Δ-[Co(NH_2)(Gly-Gly-$NHCH_2CH_2S$-)sar]$_2(ClO_4)_6$·4$HClO_4$ (9)-$(ClO_4)_6$·4$HClO_4$: The procedure used was the same as that for compound **5** above. From [Co(NH_3)($NH_2CH_2CO_2H$)sar]Cl_5·3H_2O (0.50 g, 0.75 mmol), DMF (15 mL), DIPEA (0.26 mL, 1.5 mmol + 0.5 mL, 3 mmol), *N*-hydroxysuccinimide (0.17 g, 1.5 mmol), EDC·HCl (0.29 g, 1.5 mmol), Boc-Gly-CSA (0.17 g, 0.36 mmol), was obtained (**9**)$(ClO_4)_6$·4$HClO_4$ (0.21 g, 0.10 mmol). The sample was recrystallised from warm H_2O by the addition of EtOH. ^1H NMR (600 MHz, [D_6]DMSO): δ = 2.40–2.70 and 2.90–3.35 (m, 48 H, 2 cage $–CH_2–$), 2.76 (t, 4 H, 2 $–CH_2–$S), 3.24 (s, 4 H, 2 Gly_1 $–CH_2–$), 3.36 (q, 4 H, 2 CSA $–CH_2–$N), 3.74 (d, 4 H, 2 Gly_2

 © 2007 Wiley-VCH Verlag GmbH & Co. KGaA, Weinheim

–CH_2–), 6.59 (br. s, 6 H, 2 cage –NH–), 6.85 (br. s, 6 H, 2 cage –NH–), 8.01 (s, 2 H, 2 Gly_2 amide NH), 8.11 (t, 2 H, 2 CSA amide NH), 8.41 (br. s, 4 H, 2 free $–NH_2$). ^{13}C NMR (151 MHz, [D_6]DMSO): δ = 36.9 (CSA $–CH_2–S$), 37.9 (CSA $–CH_2–N$), 41.6 (Gly_2 $–CH_2–$), 44.3 (Gly_1 $–CH_2–$), 50.9, 52.1, 53.4 (2 C) (cage $–CH_2–$), 55.5, 60.4 (C), 168.7, 170.6 (C=O). ES-MS: *m*/*z* = 544.24 $[C_{40}H_{86}Co_2N_{20}O_4S_2 – 4\ H^+]^{2+}$. $C_{40}H_{90}Cl_{10}Co_2N_{20}O_{44}S_2$ [(**9**)$(ClO_4)_6$·4$HClO_4$, 2091.78]: calcd. C 22.97, H 4.34, N 13.39; found C 23.20, H 4.47, N 13.38.

Δ-[Co(NH_2)(Gly-Ala-NHCH_2CH_2S-)sar]$_2$(ClO_4)$_6$·2$HClO_4$·H_2O (10)(ClO_4)$_6$·2$HClO_4$·H_2O: The procedure used was the same as that for compound **5** above. From [Co(NH_3)($NH_2CH_2CO_2H$)-sar](CF_3SO_3)$_5$ (1.00 g, 0.85 mmol), DMF (15 mL), DIPEA (0.30 mL, 1.7 mmol + 0.50 mL, 3 mmol), *N*-hydroxysuccinimide (0.11 g, 0.96 mmol), HBTU (0.35 g, 0.92 mmol), Boc-Ala-CSA (0.20 g, 0.40 mmol), was obtained (**10**)$(ClO_4)_6$·2$HClO_4$·H_2O (0.42 g, 0.22 mmol). The sample was recrystallised from warm H_2O by the addition of EtOH. ^1H NMR (600 MHz, [D_6]DMSO): δ = 1.22 (d, 6 H, 2 Ala $–CH_3$), 2.40–2.70 and 2.85–3.40 (m, 48 H, 2 cage $–CH_2–$), 2.76 (m, 4 H, 2 $–CH_2–S$), 3.17 (AB q, 4 H, 2 Gly_1 $–CH_2–$), 3.25–3.45 (m, 4 H, 2 CSA $–CH_2–N$), 4.30 (quint, 2 H, 2 Ala_2 –CHα–), 6.54 (br. s, 6 H, 2 cage –NH), 6.80 (br. s, 6 H, 2 cage –NH), 7.85 (d, 2 H, 2 Ala_2 amide NH), 8.20 (t, 2 H, 2 CSA amide NH), 8.41 (br. s, 4 H, 2 free $–NH_2$). ^{13}C NMR (151 MHz, [D_6]DMSO): δ = 19.00 (Ala_2 $–CH_3$), 36.92 (CSA $–CH_2–S$), 37.87 (CSA $–CH_2–N$), 44.47 (Gly_1 $–CH_2–$), 47.73 (Ala_2 –CHα–), 51.20, 52.32, 53.28 (cage $–CH_2–$), 55.62, 60.34 (cage C), 169.90, 172.12 (C=O). ES-MS: *m*/*z* = 372.51 $[C_{42}H_{90}Co_2N_{20}O_4S_2 – 3\ H^+]^{3+}$, 279.64 $[C_{42}H_{90}Co_2N_{20}O_4S_2 – 2\ H^+]^{4+}$. $C_{42}H_{94}Cl_8Co_2N_{20}O_{37}S_2$ [(**10**)$(ClO_4)_6$·2$HClO_4$·H_2O, 1936.93]: calcd. C 26.04, H 4.89, N 14.46; found C 26.24, H 5.01, N 14.28.

Acknowledgments

We thank the University of Western Australia for partial funding of this research and NSERC for financial support. H.-B. K. is the Canadian Research Chair in Biomaterials. G. L. N. was the holder of an Australian Postgraduate Award. We also thank Dr. Dimitre Karpuzov, University of Alberta, for the XPS measurements.

[1] J. C. Love, L. A. Estroff, J. K. Kriebel, R. G. Nuzzo, G. M. Whitesides, *Chem. Rev.* **2005**, *105*, 1103.
[2] M.-C. Daniel, D. Astruc, *Chem. Rev.* **2004**, *104*, 293.
[3] A. M. Sargeson, *Pure Appl. Chem.* **1986**, *58*, 1511.
[4] A. M. Sargeson, *Coord. Chem. Rev.* **1996**, *151*, 89.
[5] M. H. Jensen, P. Osvath, A. M. Sargeson, J. Ulstrup, *J. Electroanal. Chem.* **1994**, *377*, 131.
[6] J. T. Hupp, H. Y. Liu, P. A. Lay, W. H. F. Petri, A. M. Sargeson, M. J. Weaver, *J. Electroanal. Chem. Interfacial Electrochem.* **1984**, *163*, 371.
[7] I. I. Creaser, A. Hammershoei, A. Launikonis, A. W. H. Mau, A. M. Sargeson, W. H. F. Sasse, *Photochem. Photobiol.* **1989**, *49*, 19.
[8] C. Konigstein, A. W. H. Mau, P. Osvath, A. M. Sargeson, *Chem. Commun.* **1997**, 423.
[9] A. Launikonis, P. A. Lay, A. W. H. Mau, A. M. Sargeson, W. H. F. Sasse, *Sci. Pap. Inst. Phys. Chem. Res. (Jpn.)* **1984**, *78*, 198.
[10] A. W. H. Mau, W. H. F. Sasse, I. I. Creaser, A. M. Sargeson, *Nouv. J. Chim.* **1986**, *10*, 589.
[11] L. R. Gahan, T. W. Hambley, A. M. Sargeson, M. R. Snow, *Inorg. Chem.* **1982**, *21*, 2699.
[12] S. Burnet, M.-H. Choi, P. S. Donnelly, J. M. Harrowfield, I. Ivanova, S.-H. Jeong, Y. Kim, M. Mocerino, B. W. Skelton, A. H. White, C. C. Williams, Z.-L. Zeng, *Eur. J. Inorg. Chem.* **2001**, 1869.
[13] A. S. Paxinos, H. Gunther, D. J. M. Schmedding, H. Simon, *Bioelectrochem. Bioenerg.* **1991**, *25*, 425.
[14] J. M. Harrowfield, G. A. Koutsantonis, G. L. Nealon, B. W. Skelton, A. H. White, *Eur. J. Inorg. Chem.* **2005**, 2384.
[15] G. W. Walker, R. J. Geue, A. M. Sargeson, C. A. Behm, *Dalton Trans.* **2003**, 2992.
[16] P. S. Donnelly, J. M. Harrowfield, B. W. Skelton, A. H. White, *Inorg. Chem.* **2000**, *39*, 5817.
[17] M. Bodanszky, A. Bodanszky, *The Practice of Peptide Synthesis*, 2nd ed., Springer Verlag, Berlin, **1994**.
[18] G. A. Orlowski, S. Chowdhury, Y.-T. Long, T. C. Sutherland, H.-B. Kraatz, *Chem. Commun.* **2005**, 1330.
[19] H.-B. Kraatz, *J. Inorg. Organomet. Polym.* **2005**, *15*, 83.
[20] D. W. Conrad, H. Zhang, D. E. Stewart, R. A. Scott, *J. Am. Chem. Soc.* **1992**, *114*, 9909.
[21] P. S. Donnelly, J. M. Harrowfield, *J. Chem. Soc., Dalton Trans.* **2002**, 906.
[22] S. F. Ralph, M. M. Sheil, L. A. Hick, R. J. Geue, A. M. Sargeson, *J. Chem. Soc., Dalton Trans.* **1996**, 4417.
[23] J. M. Harrowfield, *Supramol. Chem.* **2006**, *18*, 125 and references cited therein.
[24] A. M. Bond, G. A. Lawrance, P. A. Lay, A. M. Sargeson, *Inorg. Chem.* **1983**, *22*, 2010.
[25] K. V. Gobi, T. Okajima, K. Tokuda, T. Ohsaka, *Langmuir* **1998**, *14*, 1108.
[26] A. Ulman, *Chem. Rev.* **1996**, *96*, 1533 and references cited therein.
[27] A. J. Bard, L. R. Faulkner, *Electrochemical Methods*, 2nd ed., John Wiley & Sons, New York, **2001**.
[28] I. Bediako-Amoa, T. C. Sutherland, C.-Z. Li, R. Silerova, H.-B. Kraatz, *J. Phys. Chem. B* **2004**, *108*, 704.
[29] E. Laviron, *J. Electroanal. Chem.* **1979**, *100*, 263.
[30] H. Matsuda, K. Aoki, K. Tokuda, *J. Electroanal. Chem.* **1987**, *217*, 15.
[31] T. Ishida, N. Choi, W. Mizutani, H. Tokumoto, I. Kojima, H. Azehara, H. Hokari, U. Akiba, M. Fujihira, *Langmuir* **1999**, *15*, 6799.
[32] A. A. Achilleos, L. R. Gahan, T. W. Hambley, P. C. Healy, D. M. Weedon, *Inorg. Chim. Acta* **1989**, *157*, 209.
[33] Y. Okamoto, H. Nakano, T. Imanaka, S. Teranishi, *Bull. Chem. Soc. Jpn.* **1975**, *48*, 1163.
[34] R. J. Geue, T. W. Hambley, J. M. Harrowfield, A. M. Sargeson, M. R. Snow, *J. Am. Chem. Soc.* **1984**, *106*, 5478.
[35] S. Chowdhury, G. Schatte, H.-B. Kraatz, *Dalton Trans.* **2004**, 1726.
[36] S. R. Hall, D. J. Du Boulay, R. E. Olthof-Hazekamp, XTAL 3.7, The University of Western Australia, **2001**.

Received: May 3, 2006
Published Online: November 9, 2006

 © 2007 Wiley-VCH Verlag GmbH & Co. KGaA, Weinheim